THE ASTROPHYSICAL JOURNAL, 396:311–332, 1992 September 1

THE INFLUENCE OF A VERTICAL MAGNETIC FIELD ON OSCILLATIONS IN AN ISOTHERMAL STRATIFIED ATMOSPHERE

S. S. HASAN
Harvard-Smithsonian Center for Astrophysics, 60 Garden Street, Cambridge, MA 02138;
and Indian Institute of Astrophysics, Bangalore 560 034, India

AND

J. CHRISTENSEN-DALSGAARD
Institut for Fysik og Astronomi, Aarhus Universitet, DK-800 C, Denmark
Received 1991 December 16; accepted 1992 March 9

ABSTRACT

We examine the effect of a uniform vertical magnetic field on the modes of an isothermal stratified atmosphere. The general solutions of the wave equation for an isothermal magnetized medium are first given. We present asymptotic expansions of these solutions in the strong- and weak-field limits. In the latter case, an analytical expression for the dispersion relation is derived, which allows the effect of a weak magnetic field on the modes to be studied. For a weak field we find that, to lowest order in our perturbation expansion, the oscillation spectrum can be analysed in terms of (*a*) *p*- and *g*-like modes; (*b*) magnetic Lamb modes; and (*c*) magnetic or slow modes. Our approximation is valid as long as the frequencies of the individual modes are well separated and not too low. The frequency corrections for each of the modes due to coupling with the remaining modes are calculated. It is explicitly demonstrated that when the frequencies of different modes are almost identical, strong mode coupling occurs and the waves acquire a mixed character. At such frequencies, the asymptotic behavior cannot be treated in terms of elementary modes, but has to be modified to include the effects of degeneracy. An analysis of the solutions in the vicinity of the degenerate frequencies is carried out. Detailed results are presented in the form of diagnostic diagrams, showing the variation of frequency with horizontal wave number. The solutions clearly reveal the presence of *avoided crossings*, which occur at the otherwise degenerate frequencies. Examples of different types of avoided crossings are given. We also present results for the moderate to strong field case and identify the solutions of various orders. A comparison is made with previous studies.

Subject headings: MHD — Sun: oscillations

1. INTRODUCTION

Magnetic fields dominate the structure of the solar surface layers, and the existence of magnetic fields in other stars has been confirmed by several observations. For instance, it is well known that the solar photosphere is permeated with vertical magnetic fields, usually in the form of flux tubes. Examples of these range from fibrils or intense flux tubes, which constitute the small-scale magnetic field, to sunspots, which play an important role in global solar activity. A study of wave motions can reveal useful information on the structure of magnetic elements and thus serve as a powerful diagnostic tool. Indeed, oscillations with periods in a fairly broad range of frequencies have been widely reported in magnetic elements. Examples of these are umbral oscillations (Beckers & Schulz 1972; Bhatnagar, Livingston, & Harvey 1972; Rice & Gaizauskas 1973; Schröter & Soltau 1976; von Uexküll et al. 1983; Lites 1984; Lites & Thomas 1985; Abdelatif, Lites, & Thomas 1984, 1986; Balthasar, Küveler, & Wiehr 1987; Gurman 1987; see also the review by Moore & Rabin 1985). Apart from the observations of Giovanelli (1975) and Giovanelli, Harvey, & Livingston (1978) few data are available on oscillations in fibrils, due to their small horizontal dimensions. Given the large amount of observational evidence on the existence of oscillations in magnetic elements, it is natural to seek a theoretical explanation of the various wave modes that can occur in them. Any theory has to take into account the variable structure of the atmosphere in the vertical direction. As a first step, one can use local dispersion relations (e.g., McLellan & Winterberg 1968; Bel & Mein 1971; Nagakawa, Priest, & Wellck 1973), which provide a qualitative description of the oscillations. In particular, this method demonstrates the existence of cutoffs in the propagation frequency. However, for comparing theoretical results with observations, global dispersion relations must be used. Indeed, it has been found that the local approach, based upon the WKB approximation, can give misleading results (Thomas 1982).

Thus, what is required is a theory of wave propagation in a stratified atmosphere with a vertical magnetic field. The theoretical understanding of the nature of wave modes in such a medium is currently far from complete, despite the existence of a large number of papers on the subject (e.g., Ferraro & Plumpton 1958, hereafter FP; Uchida & Sakurai 1975; Antia & Chitre 1978; Zhugzhda 1979; Scheuer & Thomas 1981; Leroy & Schwartz 1982; Zhugzhda & Dzhalilov 1982, hereafter ZD, 1984a, 1984b; Hasan & Sobouti 1987; Hasan & Abdelatif 1990; Abdelatif 1990; Hasan 1991; see also the reviews by Thomas 1983; Roberts 1985; Campos 1987; Hollweg 1990). This is principally because the theory of magneto-acoustic-gravity (hereafter abbreviated as MAG) waves is rather complicated. Analytic progress has generally been confined to special cases, such as assuming an isothermal stratification. This case was examined in some detail by FP, who obtained asymptotic solutions of the wave equations in the limits of strong and weak magnetic fields for an isothermal plasma. The analysis was carried further by Zhugzhda (1979) and ZD to treat the more

general case of arbitrary field strength. The latter authors were able to obtain the exact solution of the wave equation in terms of Meijer functions. Despite this mathematical progress, the physical properties of the solutions have not been fully explored. The stratification allows mutual transformation of waves, so that in general the problem cannot be examined in terms of the elementary modes of a nonstratified magnetized atmosphere.

In this investigation, we attempt to analyse the physical nature of MAG oscillations, by examining how the normal modes of an unmagnetized stratified atmosphere are modified by the introduction of a small vertical magnetic field. Some aspects of this problem have been studied in the past among others by Ledoux & Simon (1957), Goosens (1972), Goosens, Smeyers, & Denis (1976), Biront et al. (1982), and Roberts & Soward (1983). These investigations used a perturbation approach to treat the effect of a magnetic field on radial oscillations. In the present study, we shall be concerned primarily with nonradial modes (i.e., modes with finite horizontal wave number). New features present in our analysis include a calculation of the frequency shift of the p- and g-modes of an unmagnetized atmosphere due to the presence of a vertical magnetic field, the explicit demonstration of the existence of a magnetic Lamb mode and a treatment of the interaction of magnetic modes with nonmagnetic modes. The calculation of the frequency shifts of p-modes due to a *horizontal* (or toroidal) magnetic field has been carried out by several authors such as Dziembowski & Goode (1984), Gough & Taylor (1984), Roberts & Campbell (1986), Gough & Thompson (1988, 1990), Vorontsov (1988), and Campbell & Roberts (1989). However, an investigation of the frequency shifts of p-modes for a vertical field in a stratified atmosphere has so far received practically no attention, largely due to the fact that the order of the relevant differential equation changes from two (for an unmagnetized or horizontal field) to four (for a vertical field).

For vertical fields, the effect on p-mode frequencies due to scattering off flux tubes has been addressed by Zweibel & Bogdan (1987), Bogdan & Zweibel (1987), and Bogdan & Cattaneo (1989), but the stratification was neglected in these studies. Mode coupling in a stratified atmosphere with a strong magnetic field has been studied by Hasan & Abdelatif (1990) and Abdelatif (1990), and in a general field by Spruit & Bogdan (1992). Abdelatif (1990) elucidated the frequency behavior in the $K - \Omega$ diagram in the strong-field case, showing that it could be understood, for small horizontal wave numbers, in terms of the interaction between fast and slow modes. The present study considers both the strong- and weak-field solutions of the wave equation, with the main emphasis on the latter. In the strong-field limit, our results complement those of Abdelatif (1990) by using the small and large horizontal wave number limits to classify the modes. Our investigation differs from that of Spruit & Bogdan (1992) in two important respects: in the assumed temperature stratification of the atmosphere, and, more importantly, in the methods employed in the analysis of the problem. The primary concern of Spruit & Bogdan was to find a mechanism for converting p-modes into downward propagating slow waves, in order to explain p-mode absorption in a sunspot. In contrast, we concentrate on examining the normal modes of the system, by combining a semi-analytic approach based on asymptotic dispersion relations, with numerical solutions; in this way, it is possible to examine the nature of modes and gain an understanding of their mutual interaction in a vertical magnetic field.

Strictly speaking, the present analysis pertains to homogeneous fields and not to flux tubes. Unfortunately, even the construction of an equilibrium solution for a stratified flux tube is extremely complicated, let alone the question of wave propagation. Most of the analyses of waves in flux tubes have either neglected gravity or used the thin flux tube approximation (see Hollweg 1990; Roberts 1990; Thomas 1990 for recent reviews on flux tube waves). The former approach, which neglects the stratification, is inappropriate for application to photospheric flux tubes. The thin flux tube approximation, on the other hand, provides a more reasonable framework for treating wave propagation in intense flux tubes, where the tube radius is typically smaller than the pressure scale height in the vertical direction. However, in addition to its somewhat restrictive scope, this approximation has the limitation that it effectively eliminates the fast mode from the analysis. In the present investigation, it is assumed that the flux tubes in question are sufficiently thick, so that the field can be regarded to have infinite horizontal extent. Furthermore, we employ a set of boundary conditions, which may not be directly applicable to a realistic solar situation; nevertheless, the results provide some insight into the general properties of oscillations in a stratified atmosphere with a vertical magnetic field.

The plan of the paper is as follows: in § 2, the basic wave equations are presented for an isothermal stratified atmosphere in a vertical magnetic field. This is followed in §§ 3 and 4 by an analysis of the asymptotic solutions in the limits of vanishing and infinite horizontal wave number respectively. In § 5 we present the dispersion relation for a weak field. We show that the normal-mode frequency can be expressed as the sum of an elementary-mode frequency and a first-order correction, due to coupling between the different modes. We also examine the behavior of the solutions close to the degenerate frequencies, i.e., when the different elementary modes have the same frequency. In §§ 6 and 7, numerical results are presented showing the variation of the eigenfrequencies with horizontal wave number, for both weak and moderate field strengths. A discussion of the results and a comparison with previous studies is taken up in § 8. Finally, the salient features of this investigation and the main conclusions are summarized in § 9.

2. WAVE EQUATIONS IN A UNIFORM VERTICAL FIELD

We consider an isothermal stratified atmosphere, with a uniform vertical magnetic field B, which is unbounded in the horizontal direction. In Cartesian geometry, the linearized equations for MAG waves can be written in terms of the Lagrangian displacement $\xi \sim e^{i(\omega t - kx)}$ as (Ferraro & Plumpton 1958)

$$\left[v_A^2 \frac{d^2}{dz^2} - (c_S^2 + v_A^2)k^2 + \omega^2\right]\xi_x - ik\left(c_S^2 \frac{d}{dz} - g\right)\xi_z = 0 , \tag{1}$$

$$\left[c_S^2 \frac{d^2}{dz^2} - \gamma g \frac{d}{dz} + \omega^2\right]\xi_z - ik\left[c_S^2 \frac{d}{dz} - (\gamma - 1)g\right]\xi_x = 0 , \tag{2}$$

$$\left(\omega^2 + v_A^2 \frac{d^2}{dz^2}\right)\xi_y = 0 , \tag{3}$$

where z, the vertical coordinate, is measured positive upward, k is the horizontal wavenumber, ω is the frequency, g is the acceleration due to gravity, γ is the ratio of specific heats, c_S is the sound speed and v_A is the Alfvén speed. The sound and Alfvén speeds are defined respectively as

$$c_S = \sqrt{\frac{\gamma p}{\rho}} \quad \text{and} \quad v_A = \frac{B}{\sqrt{4\pi\rho}},$$

where p is the gas pressure and ρ is the mass density. Equations (1) and (2) govern the propagation of MAG waves in a stratified atmosphere.

Equation (3), which, incidentally, is decoupled from the other equations and describes the purely transverse Alfvén waves, will not be considered in the present investigation. Detailed solutions for Alfvén waves in an isothermal plasma can be found in the paper by FP. We have implicitly assumed that the propagation and motions of the MAG modes are confined to the $x - z$ plane. This involves no loss of generality.

For simplicity, let us assume that the equilibrium atmosphere is isothermal. This implies that c_S is constant with z and that ρ has the following height dependence

$$\rho = \rho_0 e^{-z/H}, \tag{4}$$

where H is the scale height of the atmosphere.

It is convenient to work in terms of the following dimensionless parameters

$$K = kH, \tag{5a}$$

$$\Omega = \frac{\omega H}{c_S}, \tag{5b}$$

and the dimensionless vertical coordinate

$$\theta = \frac{\omega H}{v_A} = \frac{c_S}{v_{A,0}} \Omega e^{-z/(2H)}, \tag{5c}$$

where $v_{A,0}$ is the Alfvén speed at $z = 0$. In terms of the variables defined by equations (5a)–(5c), equations (1)–(2) can be combined into the following fourth-order differential equation for ξ_x (Zhugzhda 1979)

$$\left[\theta^4 \frac{d^4}{d\theta^4} + 4\theta^3 \frac{d^3}{d\theta^3} + [1 + 4(\Omega^2 - K^2) + 4\theta^2]\theta^2 \frac{d^2}{d\theta^2} - [1 - 4(\Omega^2 + K^2) - 12\theta^2]\theta \frac{d}{d\theta} + 16\left\{\left[\Omega^2 + K^2\left(\frac{\Omega_{BV}^2}{\Omega^2} - 1\right)\right]\theta^2 - \Omega^2 K^2\right\}\right]\xi_x = 0, \tag{6}$$

where $\Omega_{BV}^2 = (\gamma - 1)/\gamma^2$ is the squared Brunt-Väisälä frequency (in dimensionless units). The general solution of equation (6), which can be expressed in terms of Meijer functions (ZD) is given in Appendix A, along with the asymptotic expansions in the strong and weak field limits.

For physical reasons and also for purposes of mode classification it is instructive to consider first the limiting cases $K \to 0$ and $K \to \infty$.

3. SOLUTIONS FOR $K \to 0$

From equations (1)–(2), we find that in the limit $K = 0$, ξ_x and ξ_z become decoupled. It is fairly straightforward to see that as $K \to 0$, there are two sets of solution

$$\xi_x = c_1 J_0(2\theta) + c_2 Y_0(2\theta), \quad \xi_z = 0, \tag{7}$$

$$\xi_z = c_2 \theta^{-1+i\alpha} + c_4 \theta^{-1-i\alpha}, \quad \xi_x = 0, \tag{8}$$

where $\alpha = (4\Omega^2 - 1)^{1/2}$, c_i ($i = 1, 2, \ldots, 4$) are constants, and J_0 and Y_0 are the Bessel functions. It should be noted that the above solutions are valid for arbitrary field strengths. In the limit of a weak magnetic field, for which $\theta \gg 1$, the asymptotic form of the solutions in equations (7) and (8) can be identified with the general asymptotic solution derived in Appendix A. Thus, the asymptotic limit of equation (7) essentially corresponds to the leading-order terms in f_3 and f_4 (see eqs. [A24] and [A25]), which can be recognized as the magnetic contributions to the solution and physically correspond to slow MHD waves. Similarly, in this limit the solution in equation (8) corresponds to the leading-order term of f_1 and f_2 as defined in equations (A22) and (A23); it is recognized as the usual p- or acoustic mode in an unmagnetized plasma and represents a vertically propagating wave when Ω exceeds the acoustic cutoff frequency Ω_a (which in dimensionless units is $\frac{1}{2}$). This solution is unaffected by the magnetic field.

4. SOLUTIONS FOR $K \to \infty$

In the limit $K \to \infty$, it can be easily seen that equations (1) and (2) reduce to the following differential equation (Moreno-Insertis & Spruit 1989; see also the derivation in Roberts & Small 1990)

$$\frac{d^2\xi_z}{dz^2} - \frac{1}{H}\frac{c_T^2}{c_S^2}\frac{d\xi_z}{dz} + \frac{1}{H^2}\frac{c_S^2}{c_T^2}\left[\Omega^2 - \frac{c_T^2}{v_A^2}\left(\Omega_{BV}^2 + \frac{c_T^2}{\gamma c_S^2}\right)\right]\xi_z = 0, \tag{9}$$

where c_T denotes the tube speed given by

$$c_T^2 = \frac{c_S^2 v_A^2}{c_S^2 + v_A^2} . \tag{10}$$

When $c_S/v_A \gg 1$, $c_T \to v_A$ and equation (9) becomes

$$\frac{d^2\xi_z}{dz^2} + \frac{1}{H^2}\frac{c_S^2}{v_A^2}(\Omega^2 - \Omega_{BV}^2)\xi_z = 0 . \tag{11}$$

Equation (11) admits the solutions

$$\xi_z = d_1 J_0(\psi) + d_2 Y_0(\psi) , \tag{12}$$

where d_1 and d_2 are constants and

$$\psi = 2\frac{\theta}{\Omega}\sqrt{\Omega^2 - \Omega_{BV}^2} . \tag{13}$$

For propagating wave solutions, $\Omega > \Omega_{BV}$. Such solutions correspond essentially to MHD waves, modified by gravity. They will be discussed in greater detail in § 5.2.3.

5. NORMAL MODES IN A WEAK MAGNETIC FIELD

We now examine the properties of waves and normal modes of a stratified atmosphere with a weak magnetic field (corresponding to the limit of small ϵ, where $\epsilon = v_{A,0}/c_S$), in order to delineate the influence of the field on the oscillation spectrum.

In order to get a physical picture of the solutions, let us consider the case of waves propagating upward, which are excited from below at $z = 0$, in an atmosphere that is not necessarily isothermal. To the extent that their local behavior can be approximated using an isothermal treatment, the solutions can be analyzed, to lowest order in θ, in terms of acoustic and slow MHD waves. It is well known that acoustic modes are easily reflected if the temperature of the medium changes with height (for a good discussion see Leibacher & Stein 1981). The slow mode can be reflected due to the increasing Alfvén speed with height from layers where $v_A \sim c_S$, through conversion into a fast mode (e.g., Zhugzhda 1984). Although our analysis pertains to an isothermal medium with a weak field, we implicitly assume that the properties of the atmosphere change abruptly at the top boundary, resulting in downward reflection of the waves. The lower boundary condition is chosen to simulate a forcing layer at $z = 0$. This leads us to use perfectly reflecting boundary conditions; although certainly an idealization, made for mathematical convenience, this choice serves to bring out the physical properties of modes in a stratified atmosphere with a vertical field. The question of alternative boundary conditions will be addressed in § 7.

5.1. *Normal Modes*

In accordance with the preceding discussion we shall use the boundary conditions

$$\xi_x = \xi_z = 0 \quad \text{at} \quad z = 0 \quad \text{and} \quad z = d , \tag{14}$$

to isolate normal modes of the system; here d is the height of the top boundary, and we also introduce the dimensionless height $D = d/H$.

The asymptotic form of the general solution in the limit of a weak field is presented in Appendix A. Substituting the boundary conditions given by equation (14) into equations (A19) and (A30) yields the following dispersion relations (for details of the derivation see Appendix B)

$$(\Omega^2 - K^2)\sin\tilde{\theta}\sin(K_z D) = 2\frac{\epsilon}{\Omega}e^{D/4}\left\{K_z K^2\left[\cosh\left(\frac{D}{4}\right)\cos\tilde{\theta}\cos(K_z D) - 1\right]\right.$$
$$\left. + \sinh\left(\frac{D}{4}\right)\cos\tilde{\theta}\sin(K_z D)\left[M(\Omega^2 - K^2) - K^2\left(\frac{1}{\gamma} - \frac{1}{2}\right)\right]\right\} + O\left(\frac{\epsilon^2}{\Omega^2}\right), \tag{15}$$

where

$$K_z^2 = \Omega^2 - K^2\left(1 - \frac{\Omega_{BV}^2}{\Omega^2}\right) - \frac{1}{4} , \tag{16}$$

$$M = K^2\frac{\Omega_{BV}^2}{\Omega^2} - \frac{1}{16} , \tag{17}$$

$$\theta_0 = \theta(0) , \qquad \theta_D = \theta(D) , \qquad \tilde{\theta} = 2(\theta_0 - \theta_D) .$$

In Appendix B, the coefficient of the second-order term is also provided. For $\epsilon \ll \Omega$, the dispersion relation to lowest order in ϵ/Ω becomes

$$(\Omega^2 - K^2)\sin\tilde{\theta}\sin(K_z D) = 0 . \tag{18}$$

Equation (18) admits the following solutions

$$\sin (K_z D) = 0 , \tag{19a}$$

$$\Omega = K , \tag{19b}$$

$$\sin \tilde{\theta} = 0 . \tag{19c}$$

We first consider the solution given by equation (19a) which implies that $K_z D = n\pi$, where n is an integer and denotes the order of the mode. Using equation (16) yields the usual relation for p- and g-modes:

$$\Omega_i^4 - \Omega_i^2(K_t^2 + \tfrac{1}{4}) + K^2\Omega_{\rm BV}^2 = 0 \qquad (i = p, g) , \tag{20}$$

where $K_t^2 = K_z^2 + K^2$.

The solution corresponding to equation (19b) can easily be recognized as the Lamb wave in an unmagnetized atmosphere (Lamb 1932). We denote its frequency by $\Omega_{\rm L}$. This is simply a horizontally-propagating sound wave, which is evanescent in the vertical direction. Strictly speaking, the Lamb solution is not a normal mode of the atmosphere in the absence of a magnetic field, since it does not satisfy the boundary conditions given by equation (14). However, in the presence of a weak field, this can be achieved through a slight coupling with the magnetic modes.

Turning our attention to the solutions given by equation (19c), we find that these modes arise solely due to the presence of the magnetic field. The magnetic modes, hereafter referred to as m-modes, have frequencies

$$\Omega_m = \frac{\epsilon l \pi}{2s} \qquad (l = 1, 2, \ldots) , \tag{21}$$

where $s = (1 - e^{-D/2})$. The frequencies given by equation (21) agree with those obtained from the exact solution, i.e., equation (7) valid for $K = 0$, in the limit $\theta \gg 1$. These modes are approximately transverse, since it can be shown from equations (A19) and (A30) that

$$\frac{\xi_x^{(1,2)}}{\xi_z^{(1,2)}} \sim O(\theta) .$$

Physically, these modes can be interpreted as gravity-modified slow modes in a weak magnetic field.

5.2. *Asymptotic Frequency Corrections*

We now consider the corrections to the lowest order frequencies obtained from equation (18).

5.2.1. *Frequency Correction to the p- and g-Modes*

We write

$$\Omega = \Omega_i + \delta\Omega_i , \tag{22}$$

where Ω_i $(i = p, g)$ is the solution of equation (19a), and $\delta\Omega_i$ denotes the first-order correction to Ω due to the magnetic field. Substituting equation (22) in the dispersion relation (eq. [15]) yields an expression for $\delta\Omega_i$, which is

$$\delta\Omega_i = \frac{2\epsilon e^{D/4} K_z^2 K^2}{D\Omega_i^2(\Omega_i^2 - K^2)\sin\tilde{\theta}} \left(1 - \frac{K^2\Omega_{\rm BV}^2}{\Omega_i^4}\right)^{-1} \left[\cosh\left(\frac{D}{4}\right)\cos\tilde{\theta} - (-1)^n\right] , \tag{23}$$

where $K_z = n\pi/D$.

It is evident that equation (23) is singular at frequencies such that $\sin\tilde{\theta} = 0$, i.e., where the frequencies of the p- or g-modes cross the frequencies of the m-modes. As the frequency spacing between magnetic modes is proportional to ϵ (see eq. [21]), mode crossing will occur frequently when ϵ is small. As an example, Figure 1*a* shows the frequency of the p-mode with $n = 1$ evaluated from equations (22) and (23), in an atmosphere with $\epsilon = 0.01$ and $D = 1$. To illustrate more clearly the behavior near the singularity, Figure 1*b* shows $\delta\Omega_p$. At relatively low wavenumber, the region in K which is strongly influenced by the singularities is relatively small compared to the region where they have marginal influence, and where therefore equation (23) can be used to determine the frequency corrections. On the other hand, for $K \gtrsim 1.5$ the singularities dominate the behavior of $\delta\Omega_p$. In the vicinity of the singularity the asymptotic description must take into account the presence of both types of modes. We return to the treatment of this case in § 5.3; also, § 8 presents a comparison between the asymptotic behavior and the numerical results.

In the limit $K \to 0$, $\Omega_g \to 0$ and $\Omega_p \to n\pi/D$ (for $n\pi/D \gg 1$). The correction to Ω_p in this limit is

$$\delta\Omega_p = \frac{2\epsilon D e^{D/4} K^2}{n^2\pi^2 \sin\tilde{\theta}} \left[\cosh\left(\frac{D}{4}\right)\cos\tilde{\theta} - (-1)^n\right] . \tag{24}$$

The frequency correction, for small K varies as K^2 and n^{-2}, becoming negligibly small for high orders. In the limit $K \to 0$, equation (23) cannot be used for the g-modes since these have very small frequencies ($\Omega_g \sim K$).

Consider now the limit of large K, so that $K \gg \Omega$ and $K \gg K_z$. In this limit, $\Omega_g \to \Omega_{\rm BV}$ and

$$\delta\Omega_g = \frac{2\epsilon e^{D/4} n^2\pi^2}{D^3 K^2 \sin\tilde{\theta}} \left[\cosh\left(\frac{D}{4}\right)\cos\tilde{\theta} - (-1)^n\right] . \tag{25}$$

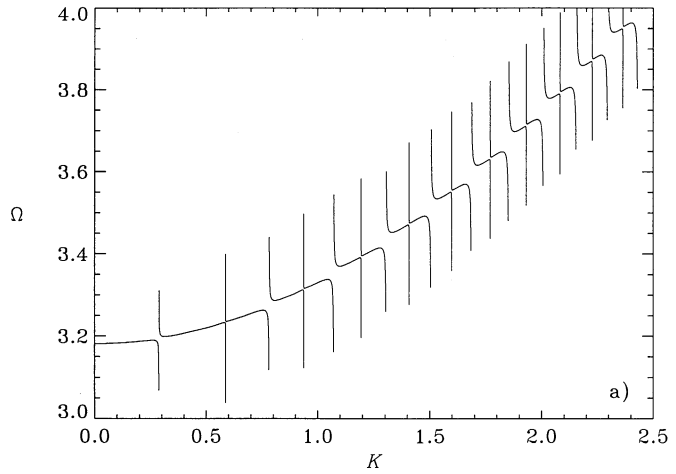

FIG. 1a

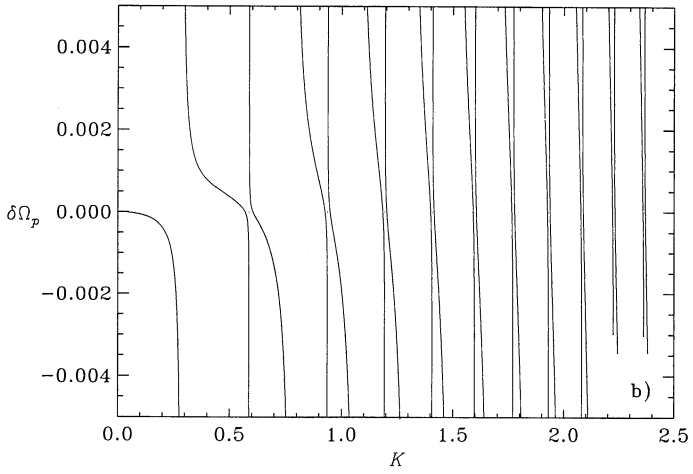

FIG. 1b

FIG. 1.—(*a*) Frequency of the p_1-mode in an atmosphere with $\epsilon = 0.01$, $D = 1$, and $\gamma = 5/3$, evaluated from eq. (22) and the simple asymptotic correction in eq. (23). (*b*) Frequency correction $\delta\Omega_p$ for this mode, evaluated from eq. (23).

Equation (25) hold for K in the range $\Omega \ll K \ll \Omega_{BV}^{3/2}\epsilon^{-1/2}$. The frequency correction for large K varies as K^{-2} and n^2, and hence increases with mode order. For larger values of K, the asymptotic solution to equation (10) can be used. This will be considered in § 5.2.3.

The correction to Ω_p cannot be obtained from equation (23) in this limit, since here $\Omega_p \sim K$.

5.2.2. *Frequency Correction to Lamb Mode*

Let us now consider the frequency correction to the Lamb mode with frequency $\Omega_L = K$. The frequency correction to this mode is

$$\delta\Omega_L = \frac{\epsilon e^{D/4}\tilde{K}_z}{\sin\tilde{\theta}\sinh(\tilde{K}_z D)}\left\{\cos\tilde{\theta}\cosh\left[\left(\frac{3}{4}-\frac{1}{\gamma}\right)D\right]-1\right\}+O\left(\frac{\epsilon^2}{K}\right), \tag{26}$$

where $\tilde{K}_z = (1/\gamma - \frac{1}{2})$. Equation (26) is valid for $K \gg \epsilon$ for small or moderate K. However, when K becomes large, the second-order correction instead varies as $\epsilon^2 K$. Thus, equation (26) is valid in the range $\epsilon^{-1} \gg K \gg \epsilon$.

As in the case of the p- and g-modes, the correction is singular at the intersections with m-modes. Figure 2 shows $\Omega_L + \delta\Omega_L$, for the same model parameters as in Figure 1. It is evident that for the Lamb mode the singularities dominate essentially everywhere. Hence equation (26), while formally correct, may be of little practical use. An asymptotic description which takes into account the interaction with the magnetic modes is discussed in § 5.3.

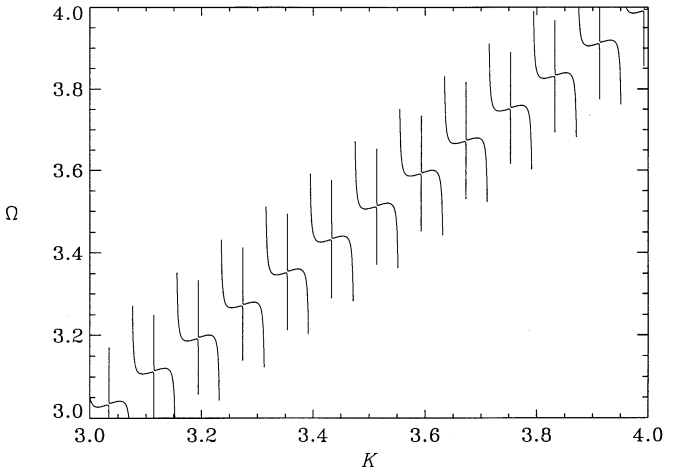

FIG. 2

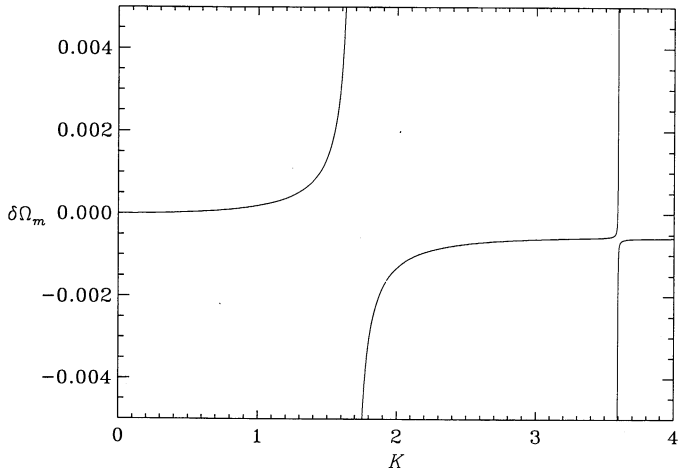

FIG. 3

FIG. 2.—Frequency of the Lamb mode in an atmosphere with $\epsilon = 0.01$, $D = 1$, and $\gamma = 5/3$, evaluated as $\Omega = K + \delta\Omega_L$, using the simple asymptotic expression in eq. (26) for $\delta\Omega_L$.

FIG. 3.—Frequency correction $\delta\Omega_m$ for the magnetic mode of order $l = 90$ and frequency $\Omega \simeq 3.59$, in an atmosphere with $\epsilon = 0.01$, $D = 1$, and $\gamma = 5/3$; $\delta\Omega_m$ was evaluated from the simple asymptotic expression in eq. (27).

5.2.3. *Frequency Correction to Magnetic Mode*

The frequency correction to Ω_m can be expressed as

$$\delta\Omega_m = \frac{2\epsilon e^{D/4}}{l\pi(\Omega_m^2 - K^2)} \left\{ \frac{K_z K^2}{\sin (K_z D)} \left[\cosh \left(\frac{D}{4} \right) \cos (K_z D) - (-1)^l \right] + \sinh \left(\frac{D}{4} \right) \left[M(\Omega_m^2 - K^2) - K^2 \left(\frac{1}{\gamma} - \frac{1}{2} \right) \right] \right\}, \tag{27}$$

where Ω_m is given by equation (21), and K_z by equation (16). Note that when K_z is imaginary, K_z should be replaced by $\tilde{K}_z = |K_z|$, $\sin (K_z D)$ by $\sinh (\tilde{K}_z D)$ and $\cos (K_z D)$ by $\cosh (\tilde{K}_z D)$ in equation (27).

In this case there are two types of singularities: one, where $\sin (K_z D) = 0$ and $K_z \neq 0$, corresponding to the crossing with the *p*- or *g*-modes; the other, where $\Omega_m = K$, corresponding to the crossing with the Lamb mode. This behavior is illustrated in Figure 3 which shows $\delta\Omega_m$ (again with $\epsilon = 0.01$ and $D = 1$) for the mode with $l = 90$, corresponding to an uncorrected magnetic frequency $\Omega_m \simeq 3.6$. It is evident that only a relatively small part of the region is influenced by the singularities; the behavior of the modes in the vicinity of the singularities is described in §§ 5.3.1 and 5.3.2.

In the limit $K \ll \Omega_m$, we find

$$\delta\Omega_m = \frac{\epsilon e^{D/4}}{l\pi} \left[-\frac{\sinh (D/4)}{8} + \frac{2K^2}{\Omega_m^2} \left\{ \frac{K_z}{\sin (K_z D)} \left[\cosh \left(\frac{D}{4} \right) \cos (K_z D) - (-1)^l \right] + \sinh \left(\frac{D}{4} \right) \left(\frac{1}{2} - \frac{1}{\gamma^2} \right) \right\} \right], \tag{28}$$

where $K_z = (\Omega_m^2 - \frac{1}{4})^{1/2}$. The first term on the right-hand side of equation (28), which is independent of K, can be traced to the asymptotic expansions of the solutions of equation (7). The second term, which varies as K^2, gives the frequency correction due to a finite horizontal wave number.

In the opposite limit, when $K \gg \Omega_m$, we have

$$\delta\Omega_m = \frac{\epsilon^2 e^{D/2} K^2 \Omega_{\rm BV}^2}{\Omega_m^3}. \tag{29}$$

The frequency correction given by equation (29) holds as long as $\delta\Omega_m/\Omega_m \ll 1$. This restricts the validity of equation (29) to K in the range $\Omega_m \ll K \ll \Omega_m^2 \epsilon^{-1}$ or roughly when $n\pi\epsilon \ll K \ll n^2\pi^2\epsilon$.

When $K \to \infty$, the frequencies can be obtained by applying the boundary conditions to the solutions of equation (11). Assuming that $\Omega \gg \epsilon$, we obtain

$$\Omega = \sqrt{\Omega_{\rm BV}^2 + \Omega_m^2}. \tag{30}$$

Thus, for $\Omega_m \gg \Omega_{\rm BV}$, the solutions essentially resemble *m*-waves modified by gravity. In this case, we have

$$\delta\Omega_m = \frac{\Omega_{\rm BV}^2}{2\Omega_m}. \tag{31}$$

In the opposite limit, when $\Omega_{\rm BV} \gg \Omega_m$, the character of the solutions is a gravity wave with frequency $\Omega_{\rm BV}$, modified by the magnetic field. The frequency correction to the *g*-mode is thus

$$\delta\Omega_g = \frac{\Omega_m^2}{2\Omega_{\rm BV}}. \tag{32}$$

5.3. *Behavior in Vicinity of Degenerate Modes*

As discussed above, the expressions for the frequency corrections derived in the preceding sections break down where frequencies of different types of modes are nearly degenerate. Thus, for example, in the vicinity of an *m*-mode, $\sin \tilde{\theta} \simeq 0$ and the expression (23) for the *p*- or *g*-mode frequency correction is singular. At such points an asymptotic description is required which takes into account the presence of both types of modes.

We again start from the dispersion relation (15). As discussed in the beginning of this section, to lowest order (i.e., by neglecting the right-hand side in eq. [15]) the eigenfrequencies are determined by equation (18), which leads to the solutions given by equations (19a)–(19c). Since the frequency of the *m*-mode is independent of K, whereas the frequencies of both *p*-, *g*- and Lamb modes increase with K, it is evident that the *m*-mode frequencies will cross the frequencies of the other modes. The actual behavior in the vicinity of such points is determined by the right-hand side of equation (15), which provides a coupling between the different types of modes.

5.3.1. *Crossings with p- or g-Modes*

We first consider a crossing between a *p*- or *g*-mode of order n, characterized by $K_z D = n\pi$, and a magnetic mode of order l with frequency $\Omega_m = \epsilon\pi l/2s$. From equation (16) it follows that this takes place at the point (K_{nl}, Ω_m) in the (K, Ω) diagram, where

$$K_{nl}^2 = \left(\Omega_m^2 - \frac{n^2\pi^2}{D^2} - \frac{1}{4} \right) \left(1 - \frac{\Omega_{\rm BV}^2}{\Omega_m^2} \right)^{-1} \tag{33}$$

(obviously crossings are only possible where $K_{nl}^2 > 0$). We now consider the behavior of the full dispersion relation (15) near this point, by setting

$$K = K_{nl} + \delta K, \qquad \Omega = \Omega_m + \delta\Omega, \tag{34}$$

where δK and $\delta\Omega$ are regarded as small quantities. Hence we may expand $\tilde{\theta}$ and K_z to obtain

$$\tilde{\theta} = l\pi + \frac{2s}{\epsilon}\,\delta\Omega$$

$$K_z \simeq \frac{n\pi}{D} - \frac{DK_{nl}}{n\pi}\left(1 - \frac{\Omega_{\rm BV}^2}{\Omega_m^2}\right)\delta K + \frac{D\Omega_m}{n\pi}\left(1 - K_{nl}^2\frac{\Omega_{\rm BV}^2}{\Omega_m^4}\right)\delta\Omega\,. \tag{35}$$

These expansions are substituted in the left-hand side of equation (15). The right-hand side and the factor $(\Omega^2 - K^2)$ are evaluated at (K_{nl}, Ω_m), leading to

$$(-1)^{n+l}\frac{2s}{\epsilon}(\Omega_m^2 - K_{nl}^2)\frac{D^2\Omega_m}{n\pi}\left[\left(1 - K_{nl}^2\frac{\Omega_{\rm BV}^2}{\Omega_m^4}\right)\delta\Omega - \left(1 - \frac{\Omega_{\rm BV}^2}{\Omega_m^2}\right)\delta K\right]\delta\Omega = \frac{\epsilon}{\Omega_m}e^{D/4}\frac{2n\pi}{D}K_{nl}^2\left[(-1)^{n+1}\cosh\left(\frac{D}{4}\right) - 1\right]. \tag{36}$$

Equation (36) provides a quadratic equation for $\delta\Omega$ as a function of δK. We write it as

$$(\delta\Omega)^2 - A\delta K\delta\Omega - \tfrac{1}{4}(\delta\Omega_{\rm min})^2 = 0\,, \tag{37}$$

with the solution

$$\delta\Omega = \tfrac{1}{2}A\delta K \pm \tfrac{1}{2}(A^2\delta K^2 + \delta\Omega_{\rm min}^2)^{1/2}\,. \tag{38}$$

Here

$$A = \frac{K_{nl}\Omega_m(\Omega_m^2 - \Omega_{\rm BV}^2)}{\Omega_m^4 - K_{nl}^2\Omega_{\rm BV}^2}\,, \tag{39}$$

$$(\delta\Omega_{\rm min})^2 = \frac{32\,\sinh\,(D/4)\eta^2}{D^3}\,\frac{n^2K_{nl}^2[\cosh\,(D/4) - (-1)^{n+l}]}{(\Omega_m^2 - K_{nl}^2)(\Omega_m^2 - K_{nl}^2\Omega_{\rm BV}^2/\Omega_m^2)}\,, \tag{40}$$

where $\eta = \epsilon\pi/(2s)$ is the separation between adjacent magnetic modes (see eq. [21]).

It is straightforward to show that for all p- and g-modes $(\delta\Omega_{\rm min})^2$ is positive, so that the two roots in equation (38) are always real and distinct. Thus, the coupling between the modes effectively removes the singular behavior, which arises when the frequencies of different modes become identical. This is characteristic of the so-called *avoided crossings*, which is a common phenomenon among the eigenvalues of problems having different classes of eigensolutions; a general analysis of the behavior near such an avoided crossing was given by von Neuman & Wigner (1929). Evidently $\delta\Omega_{\rm min}$ is the minimum separation between the two branches, at $\delta K = 0$. In the limit of large $|\,\delta K\,|$, $\delta\Omega \simeq 0$ in one branch, corresponding to the unperturbed magnetic mode, whereas on the second branch $\delta\Omega \simeq A\delta K$. The latter behavior can be understood by noting that $A = d\Omega/dK$, the derivative being taken along the unperturbed p- or g-mode ridge; hence the solution in equation (38) simply approximates the linear expansion of that ridge.

From equation (40) it follows that the minimum separation in the avoided crossings alternates between even and odd $n + l$. Neglecting the variation in K_{nl} and Ω_m, the ratio between the minimum separations is

$$\frac{\delta\Omega_{\rm min}^{(-)}}{\delta\Omega_{\rm min}^{(+)}} = \left[\frac{\cosh\,(D/4) - 1}{\cosh\,(D/4) + 1}\right]^{1/2} = \tanh\left(\frac{D}{8}\right). \tag{41}$$

Hence for small or moderate D avoided crossings with even $n + l$ are much narrower than crossings with odd $n + l$. It should also be noted that in terms of $\delta\hat{K} \equiv K/\eta$ and $\delta\hat{\Omega} \equiv \Omega/\eta$, the behavior of the avoided crossing is independent of ϵ, to this level of approximation. In particular, $\delta\Omega_{\rm min}$ is a fixed fraction of the separation η between adjacent magnetic modes. The behavior of minimum separation is illustrated in Figure 4*a*; which shows $\delta\Omega_{\rm min}^{(+)}/\eta$ as a function of K for $D = 1, \ldots, 3$, in the case when $\epsilon = 0.01$ and $\gamma = 5/3$. Only odd values for $n + l$ are included (see eq. [40]). We find that $\delta\Omega_{\rm min}^{(+)}/\eta$ increases sharply at small values of K, but saturates to values where the minimum frequency separation becomes comparable to or even larger than the adjacent magnetic mode frequencies. This behavior evidently reflects the fact that the validity of the asymptotic expansions becomes questionable for large D and K.

5.3.2. *Crossings with Lamb Mode*

In the vicinity of the unmodified Lamb mode, with $\Omega = K$, K_z is imaginary. Hence in equation (15) we replace K_z by $\tilde{K}_z = |\,K_z\,|$, $\sin\,(\tilde{K}_z D)$ by $\sinh\,(\tilde{K}_z D)$ and $\cos\,(K_z D)$ by $\cosh\,(\tilde{K}_z D)$. The frequencies of the unmodified magnetic modes are still given by equation (21), and hence the crossing takes place at $K = K_l = \Omega_m$; at this point $\tilde{K}_z = 1/\gamma - \frac{1}{2}$. Expanding again around this point, by writing

$$K = K_l + \delta K\,, \qquad \Omega = \Omega_m + \delta\Omega\,, \tag{42}$$

and replacing $\tilde{K}_z$ and the right-hand side by the values at the crossing, we obtain the approximate dispersion relation

$$(-1)^l\frac{4s}{\epsilon}(\Omega_m\delta\Omega - K_l\delta K)\sinh\left[\left(\frac{1}{\gamma} - \frac{1}{2}\right)D\right]$$

$$= \frac{\epsilon}{\Omega_m}e^{D/4}\left[2\left(\frac{1}{\gamma} - \frac{1}{2}\right)K_l^2\left\{(-1)^l\cosh\left(\frac{D}{4}\right)\cosh\left[\left(\frac{1}{\gamma} - \frac{1}{2}\right)D\right] - 1\right\} - 2\sinh\left(\frac{D}{4}\right)\sinh\left[\left(\frac{1}{\gamma} - \frac{1}{2}\right)D\right]K_l^2\left(\frac{1}{\gamma} - \frac{1}{2}\right)\right]$$

$$= (-1)^l\frac{2\epsilon}{\Omega_m}e^{D/4}\left(\frac{1}{\gamma} - \frac{1}{2}\right)K_l^2\left\{\cosh\left[\left(\frac{3}{4} - \frac{1}{\gamma}\right)D\right] - (-1)^l\right\}. \tag{43}$$

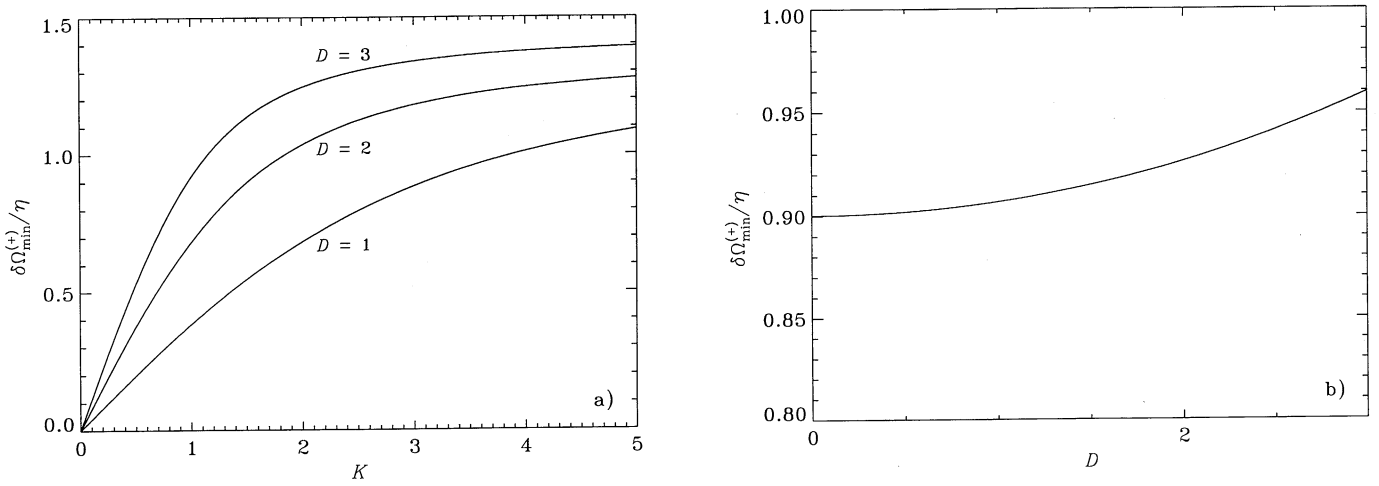

FIG. 4.—Asymptotic values for the minimum separations between adjacent avoided crossings, in units of η for $\epsilon = 0.01$, and $\gamma = 5/3$. (*a*) $\delta\Omega^{(+)}_{min}/\eta$ vs. K for $D = 1, \ldots, 3$ corresponding to the avoided crossings between the p_1 mode and magnetic modes. Only odd values of $n + l$ are included. (*b*) $\delta\Omega^{(+)}_{min}/\eta$ vs. D, for the avoided crossings between the Lamb mode and magnetic modes. Only odd values of l have been considered.

As before, this gives a quadratic equation for $\delta\Omega$, which may be written

$$(\delta\Omega)^2 - \delta K \delta\Omega - \tfrac{1}{4}(\delta\Omega_{min})^2 = 0 , \tag{44}$$

with the solution

$$\delta\Omega = \tfrac{1}{2}\delta K \pm \tfrac{1}{2}[\delta K^2 + (\delta\Omega_{min})^2]^{1/2} . \tag{45}$$

In this case

$$(\delta\Omega_{min})^2 = 16\,\frac{\eta^2}{\pi^2}\,\frac{\sinh\,(D/4)}{\sinh\,[(1/\gamma - 1/2)D]}\left(\frac{1}{\gamma} - \frac{1}{2}\right)\left\{\cosh\left[\left(\frac{3}{4} - \frac{1}{\gamma}\right)D\right] - (-1)^l\right\} , \tag{46}$$

which again is nonnegative. Hence the two roots of equation (45) are real.

As before, on one branch of the solution $\delta\Omega$ tends to 0 for large $|\delta K|$, whereas on the second $\delta\Omega \simeq \delta K$ in the limit, corresponding to the unmodified Lamb mode. Furthermore, there is again an alternation between narrow avoided crossings for even l and wide crossings for odd l, the ratio between the minimum separations in the two cases being

$$\frac{\delta\Omega^{(-)}_{min}}{\delta\Omega^{(+)}_{min}} = \left|\tanh\left[\frac{1}{2}\left(\frac{3}{4} - \frac{1}{\gamma}\right)D\right]\right| . \tag{47}$$

For the normal case of $\gamma = 5/3$, and for small or moderate D, we obtain by expanding equation (47) to leading order that $\delta\Omega^{(-)}_{min}/\delta\Omega^{(+)}_{min} \simeq 3D/40$; hence in this case also the "even" crossings are typically much narrower than the "odd" crossings. It should be noted that to this approximation $\delta\Omega^{(-)}_{min} = 0$ for the particular case of $\gamma = 4/3$, suggesting that there may be an actual degeneracy of the eigenvalues.

Figure 4*b* shows the minimum separation $\delta\Omega^{(+)}_{min}/\eta$ in an avoided crossing between the Lamb mode and a magnetic mode of odd l, as a function of D (note that $\delta\Omega^{(+)}_{min}$ is independent of K; see eq. [46]); as in Figure 4*a* separation has been normalized with the separation η between adjacent magnetic modes. The separation increases monotonically with D. Clearly, values of $\delta\Omega^{(+)}_{min}/\eta$ exceeding unity indicate a breakdown of the asymptotic description, as in the case of the separation for p-modes illustrated in Figure 4*a*.

6. $K - \Omega$ DIAGRAMS FOR A WEAK FIELD

We now present numerical results for the weak-field case. Unless otherwise stated, the atmosphere is characterized by the default values $D = 1$, $\epsilon = 0.01$, and $\gamma = 5/3$. Figure 5 shows the variation of frequency with horizontal wave number (*solid curves*) as a function of K, obtained by solving the exact equations (1) and (2) using the boundary condition (14). The solutions were computed numerically, using a fourth-order Newton-Raphson-Kantorovich scheme (Cash & Moore 1980). For comparison, we also show in Figure 5*a* results (denoted by long dashed curves) using the dispersion relation (B24). The short dashed line in that panel corresponds to the Lamb solution $\Omega = K$ and the dotted curves correspond to $g_1, \ldots, g_3$ modes in a nonmagnetic atmosphere.

Before discussing the nature of the solutions, let us first compare the numerical results with those obtained using the asymptotic expansions for the weak-field case. The two solutions are almost identical for $K < 1$. However, as K increases, the accuracy of the asymptotic solutions begins to deteriorate, the largest error occurring for the modes with lowest frequency. For $K \geq 3$, the error in the asymptotic solutions becomes fairly large for modes of low order. This is consistent with the fact that for such modes the restriction $K^2 \ll \Omega^3 v_A/c_s$ (see the discussion in Appendix A) no longer holds when K gets large.

We now turn to the properties of the solutions. The behavior at low K is illustrated in Figure 5*a*. To lowest order in ϵ, the only allowed solutions for $\Omega < 0.5$ (which is the region shown in Fig. 5*a*) consist of magnetic or m-modes, g-modes and Lamb modes. In the absence of a magnetic field, it is well known that at any given K the frequencies of the gravity modes tend to zero as the mode

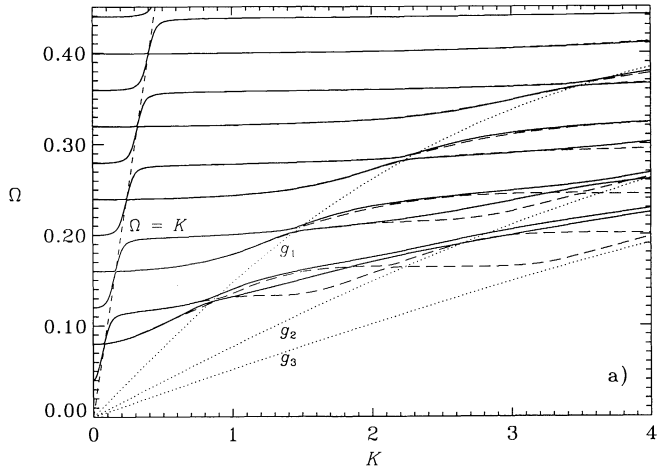

FIG. 5a

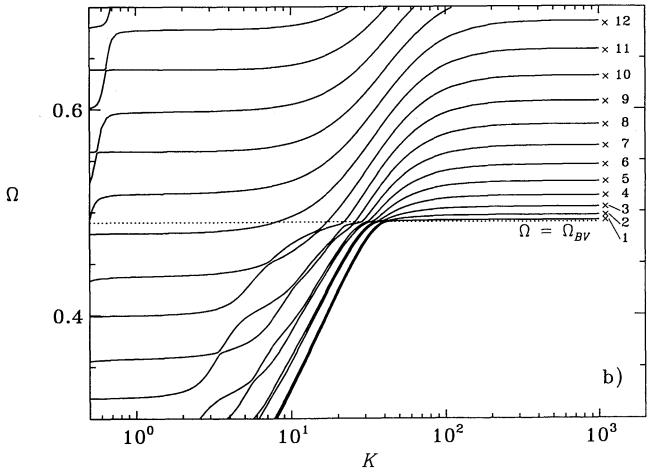

FIG. 5b

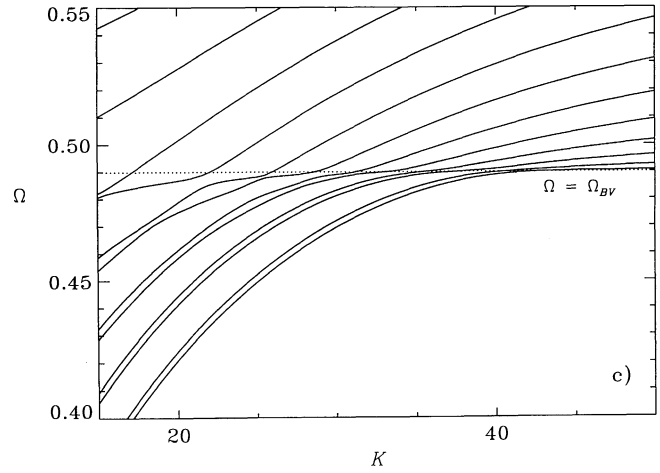

FIG. 5c

FIG. 5.—Variation of Ω with K in an isothermal atmosphere using the default values $\epsilon = 0.01$, $D = 1$ and $\gamma = 5/3$. The solid lines correspond to the numerical solution of eq. (6). In panel (*a*) the long-dashed curves are based upon the solution of the dispersion relation (B24), the short-dashed curve represents the Lamb solution $\Omega = K$, and the dotted lines correspond to the g_1, g_2, and g_3 modes in a nonmagnetic atmosphere. Panels (*b*) and (*c*) illustrate the behavior at moderate or large K. Here the dotted line shows the location of the Brunt-Väisälä frequency Ω_{BV}. In panel (*b*) the crosses mark the frequencies obtained by solving eq. (9), valid in the limit $K \to \infty$, and are labeled with the order of the corresponding modes.

order tends to infinity. Physically, this is because buoyancy, driving the g-modes, becomes increasingly inefficient as the vertical scale of the modes diminishes. Furthermore, the g-mode frequencies tend to zero as K tends to zero, because the effect of buoyancy vanishes for purely vertical propagation. The frequency of the Lamb waves also goes to zero at $K = 0$. However, in the presence of a finite magnetic field, the situation is modified. Our calculations reveal that there is a lower threshold frequency for g- and Lamb-like modes in the magnetic case, which turns out to be the frequency of the m_1 mode (the lowest-order magnetic mode). The reason for this is that the magnetic pressure driving the magnetic modes does not vanish for $K = 0$, hence adding "stiffness" to the system and preventing the frequencies from decreasing below that limit. Thus, the entire low-frequency part of the g-mode spectrum is effectively eliminated by the presence of the field. It follows that at small values of K and frequencies below those of the p-modes only m-modes are found. As K increases, however, the purely magnetic modes become modified by gravity. At frequencies at which $\Omega \simeq K$, this occurs through an interaction with the Lamb modes (modified by the magnetic field), through *avoided crossings* which we shall discuss below in greater detail when considering Figure 7. The m-modes begin to acquire a g-like character for $K \gg \Omega$. For example, the frequency of the g_1 mode exceeds that of the m_1 mode for $K \simeq 0.8$, while for the higher order g-modes, this occurs for even larger values of K. In this situation, the various modes, corresponding to equations (19a)–(19c), become coupled. As a result, the solutions for moderate K neither resemble pure m-modes nor pure g-modes, but a combination of the two.

As K is increased, there is a tendency for the two lowest modes to run in parallel with a small frequency separation. At somewhat larger values of K a similar trend develops for the next pairs of modes. (We might note that superficially similar phenomena have been obtained amongst the energy levels of a hydrogen atom in a magnetic field; see Friedrich & Wingen 1989). The change in the spectrum as K is increased even further is illustrated in Figures 5*a* and 5*b*. The character of the spectrum changes abruptly when the frequency increases beyond the Brunt-Väisälä frequency Ω_{BV} (illustrated by the dotted line) which marks the upper bound on the g-mode frequencies in the non-magnetic case. The behavior of this transition is shown in detail in Figure 5*c* as a pair of modes crosses Ω_{BV}, the apparent coupling between the modes is removed, and their frequencies increase independently. As K increases further, the frequencies tend to the values obtained from the solution of equation (9) and indicated in Figure 5*c* by crosses. The limiting frequencies can be obtained quite accurately from the asymptotic equation (30), with Ω_m given by equation (21). In particular, it might be noted that the frequency of the lowest-order model barely exceeds Ω_{BV}.

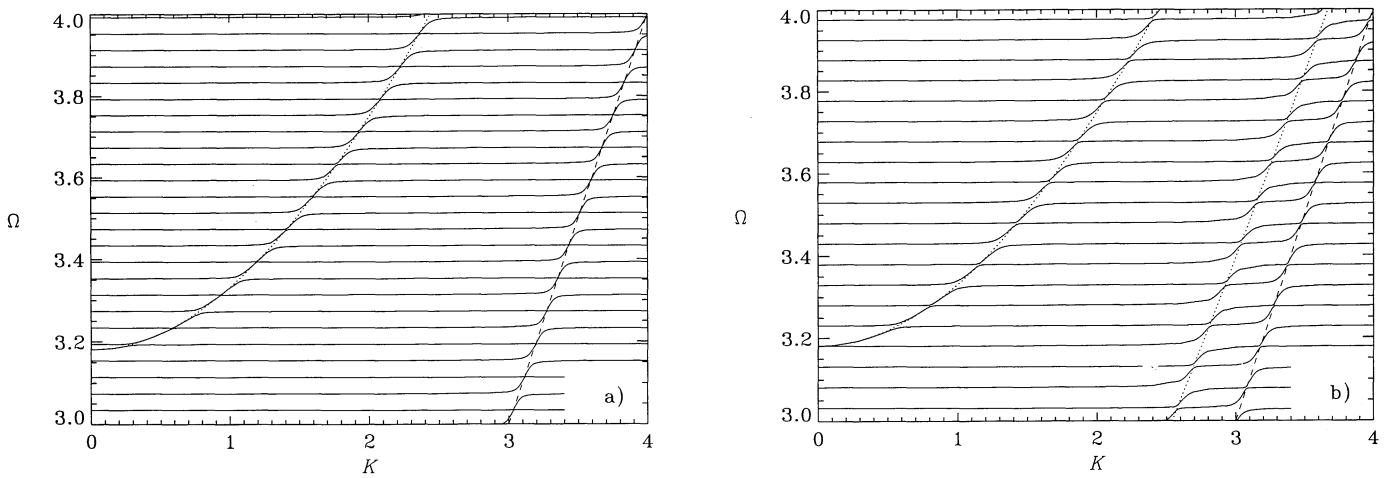

FIG. 6.—Regions in the diagnostic diagram where there are p- and Lamb-type solutions. Solid curves correspond to magnetic modes, whereas the dotted and dashed curves represent p- and Lamb modes, respectively. (*a*) Ω vs. K, using the default values for ϵ, D, and γ. The m-modes have orders between 76 and 100. Only the lowest order p-mode (p_1) is shown. (*b*) Ω vs. K for $\epsilon = 0.02$ and $D = 2$. The m-modes have orders between 61 and 80. The dotted curves show the p_1 and p_2 modes for the corresponding nonmagnetic atmosphere.

We now consider a part of the diagnostic diagram where there are p-like modes. Figure 6*a* shows the variation of Ω with K using the default values for ϵ, D, and γ. The dotted curve shows the pure p_1 mode and the dashed curve the Lamb mode ($\Omega = K$). Most of the diagnostic diagram is dominated by high-order ($l \sim 100$) magnetic modes (solid curves). However, in addition to the dense spectrum of magnetic modes, we can also discern the presence of the modified p_1 and Lamb modes. These undergo avoided crossings with various order m-modes, as discussed in greater detail in § 6.2.

Figure 6*b* shows the diagnostic diagram corresponding to the p_1, p_2 and Lamb modes for $\epsilon = 0.02$ and $D = 2$. The nonmagnetic p_1 and p_2 modes are shown as dotted lines, whereas the Lamb mode is shown as a dashed line. The behavior is very similar to that in the previous panel.

6.1. *Avoided Crossings between Lamb Mode and Magnetic Modes*

Figure 7 shows in finer detail the avoided crossings between the Lamb mode and magnetic modes at low frequencies. In the limit of $K \to 0$, the frequencies of the magnetic modes are given by the solutions of equation (7), applying the boundary condition (14); the result is

$$\Omega_{m,l} = \frac{\epsilon}{2} f_{0,l} \,, \tag{48}$$

where $f_{0,l}$ denotes the zeros of

$$J_0(2\theta_0)Y_0(2\theta_D) - J_0(2\theta_D)Y_0(2\theta_0) \,.$$

These modes have been labeled m_l ($l = 1, 2, \ldots$). The Lamb mode frequency, as mentioned above, tends to zero for $K = 0$. However,

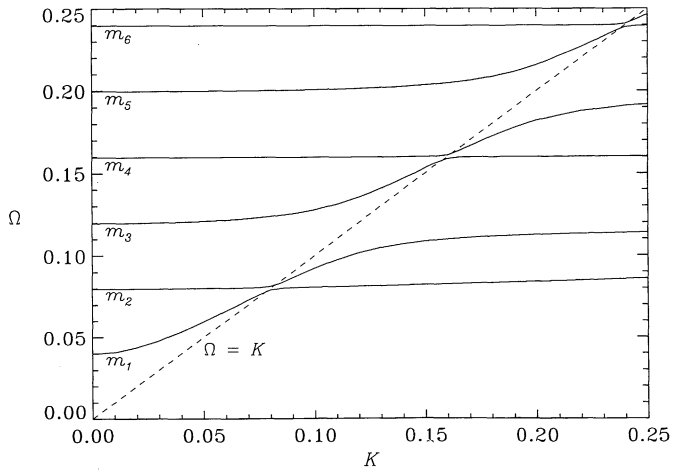

FIG. 7.—details of the avoided crossings between the magnetic modes and the Lamb mode, in the diagnostic diagram shown in Fig. 5. The magnetic modes, whose frequencies in the limit $K \to 0$ are given by the solutions of eq. (7), have been labeled $m_1, m_2, \ldots, m_6$.

for finite K the Lamb mode frequency crosses those of the magnetic modes. To investigate the resulting behavior, we focus first on the m_1 mode; as K increases, it begins to acquire the character of a magnetic Lamb mode with $\Omega \simeq K$. The m_2 mode, on the other hand, with frequency larger than that of the Lamb mode, behaves as a pure magnetic mode, with no dependence on K. As K increases further, the frequencies of the two modes approach closely. However, instead of intersecting, the two curves undergo an avoided crossing. Physically, at the avoided crossing there is strong coupling between the two modes, and the character of the solution is a mixture of a pure magnetic-like and a pure Lamb-like mode. Increasing K further leads to mode transformation, with the Lamb mode being converted into a magnetic mode and the m_2 magnetic mode becoming Lamb-like. This phenomenon is repeated again between the "new" Lamb mode and the next order magnetic mode. It is also worth noting that the crossings alternate between narrow for even l and wide for odd l, in agreement with the discussion in § 5.3.2. A similar behavior at higher frequency is clearly visible in Figure 6.

6.2. *Avoided Crossings between p-Modes and Magnetic Nodes*

Figure 8 depicts in finer detail the avoided crossings between the p_1 mode and the magnetic modes. The heavy continuous curves show the numerically computed values, whereas the asymptotic expression (38) is illustrated with thin dashed curves. We have adjusted the parameters K_{nl} and Ω_m in the asymptotic expression, in order to obtain a good fit to the numerical results. (The labeling of the computed curves is arbitrary and has been introduced for comparison with Fig. 9). The nature of the crossings is similar to that discussed in the previous section. Also, the behavior in the vicinity of the crossings is described quite accurately by the asymptotic expressions derived in § 5.3.1. In particular, the alternation between the narrow and wide separation in the crossings for even and odd $n + l$ is evident.

To illustrate the behavior of the eigenfunctions through the avoided crossings, it is instructive to consider the variation of the mode energy. We introduce

$$\tilde{E}_x = \int_0^d \xi_x^2 \exp(-z/H)dz \,, \tag{49}$$

$$\tilde{E}_z = \int_0^d \xi_z^2 \exp(-z/H)dz \,, \tag{50}$$

which are proportional to the contributions from the horizontal and the vertical velocity to the kinetic energy, respectively. Furthermore, let

$$E_z = \frac{\tilde{E}_z}{\tilde{E}_z + \tilde{E}_x} \,. \tag{51}$$

Hence E_z is the fraction of the mode energy contained in the vertical component of the velocity. For p-modes, E_z is large while it is very small for m-modes. Figure 9 shows the variation of E_z with K. The curves in the figure are labeled with the same numbering as the one used in Figure 8. For purposes of clarity each mode is distinguished by the line style in this diagram. The behavior of E_z clearly reflects the changing nature of the eigenfunction as a mode passes through an avoided crossing. For example, the mode labeled (iii) starts out as a magnetic mode with very small E_z, changes into the p_1 mode after undergoing an avoided crossing with modes (ii), and changes back again into a magnetic mode after the crossing with mode (iv).

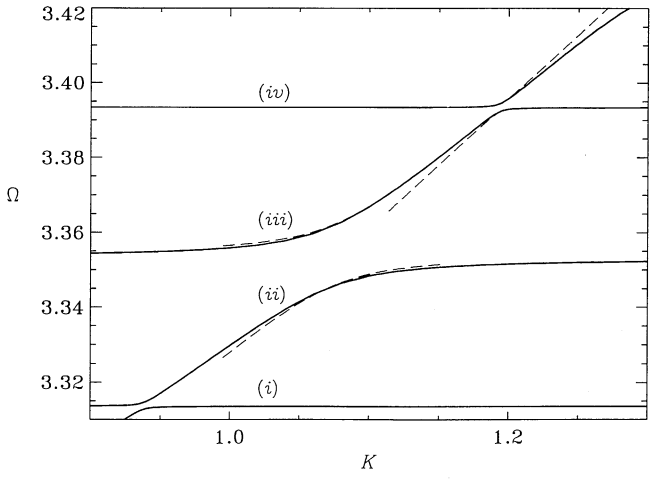

FIG. 8

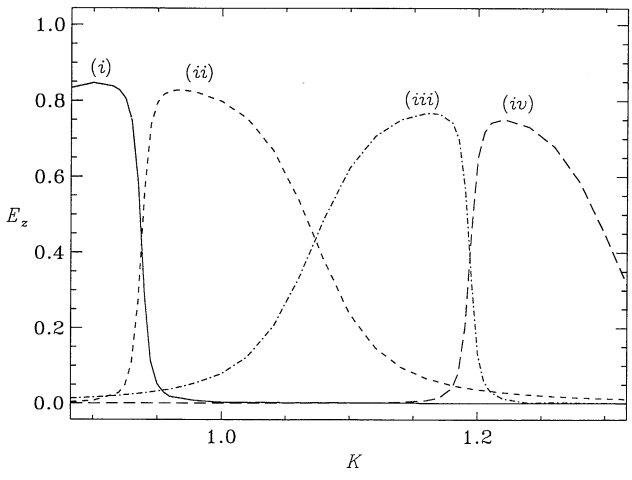

FIG. 9

FIG. 8.—Details of avoided crossings in the diagnostic diagram between the p_1 mode and the magnetic modes, for the case illustrated in Fig. 6*a*. The heavy continuous curves show the numerical solutions, whereas the asymptotic values (based upon eq. [37]) are shown by dashed curves. The curves have been labeled for purposes of comparison with Fig. 9.

FIG. 9.—Fraction of the mode kinetic energy density contained in the vertical component of the motion (see eqs. [49]–[51] vs. K, using the default parameters. The curves have been labeled using the same numbering as Fig. 8.

7. $K - \Omega$ DIAGRAMS FOR MODERATE TO STRONG FIELD

Let us now consider a situation which is more realistic as far as the solar photosphere is concerned. At the lower boundary, $v_A < c_S$, but at higher levels the Alfvén speed dominates over the sound speed. If we consider a vertical extent of several scale heights, then at the upper boundary the strong-field solutions of the wave equation corresponding to $\theta \ll 1$ given in Appendix A are applicable. Figures 10*a* and 10*b* show the diagnostic diagram corresponding to $D = 20$ for small and large values of K. The solutions were obtained by solving equation (6) numerically. The solid and dashed curves correspond to $\epsilon = 0.5$ and $\epsilon = 0.25$, respectively. An inspection of the diagnostic diagram once again reveals the presence of avoided crossings, in this case due to the interaction of p-like modes with magnetic modes.

In order to understand this behavior, we first consider the solutions for small K, shown in Figure 10*a*. We found in § 3 that for $K = 0$, there are two family of solutions, corresponding to p-modes and m-modes. The frequencies of the m-modes are given by equation (48), while the frequencies of the p-modes can be found from equation (20) with $K = 0$, i.e.,

$$\Omega_{p,n} = \sqrt{\frac{n^2\pi^2}{D^2} + \frac{1}{4}}, \tag{52}$$

where n denotes mode order. The solutions in equations (48) and (52) can be used to classify the modes close to $K = 0$ in the diagnostic diagram. In Figure 10, p_i and m_i, $(i = 1, 2, \ldots)$ denote the p- and m-modes of increasing order. The m-modes corresponding to $\epsilon = 0.25$ are denoted by $\bar{m}_i$. For sufficiently small K, the solutions consist predominantly of p-modes, interlaced with m-modes. Apart from a small horizontal layer of the atmosphere close to $z = 0$, $v_A/c_S \gg 1$, so that the spacing between the frequencies of the p-modes is smaller than that of the m-modes. For instance there are only two magnetic modes for $\epsilon = 0.5$ and four for $\epsilon = 0.25$ in the frequency range depicted in Figure 10.

The dependence of the magnetic-mode frequency on K can be understood from the so-called quasi-Alfvén approximation (Uchida & Sakurai 1975), as applied by Scheuer & Thomas (1981). It involves discarding the right-hand side of equation (A31), which is justified on the basis that $\xi_x \gg \xi_z$ in the lower atmosphere and $v_A \gg c_S$ in the upper layers of the atmosphere. In the

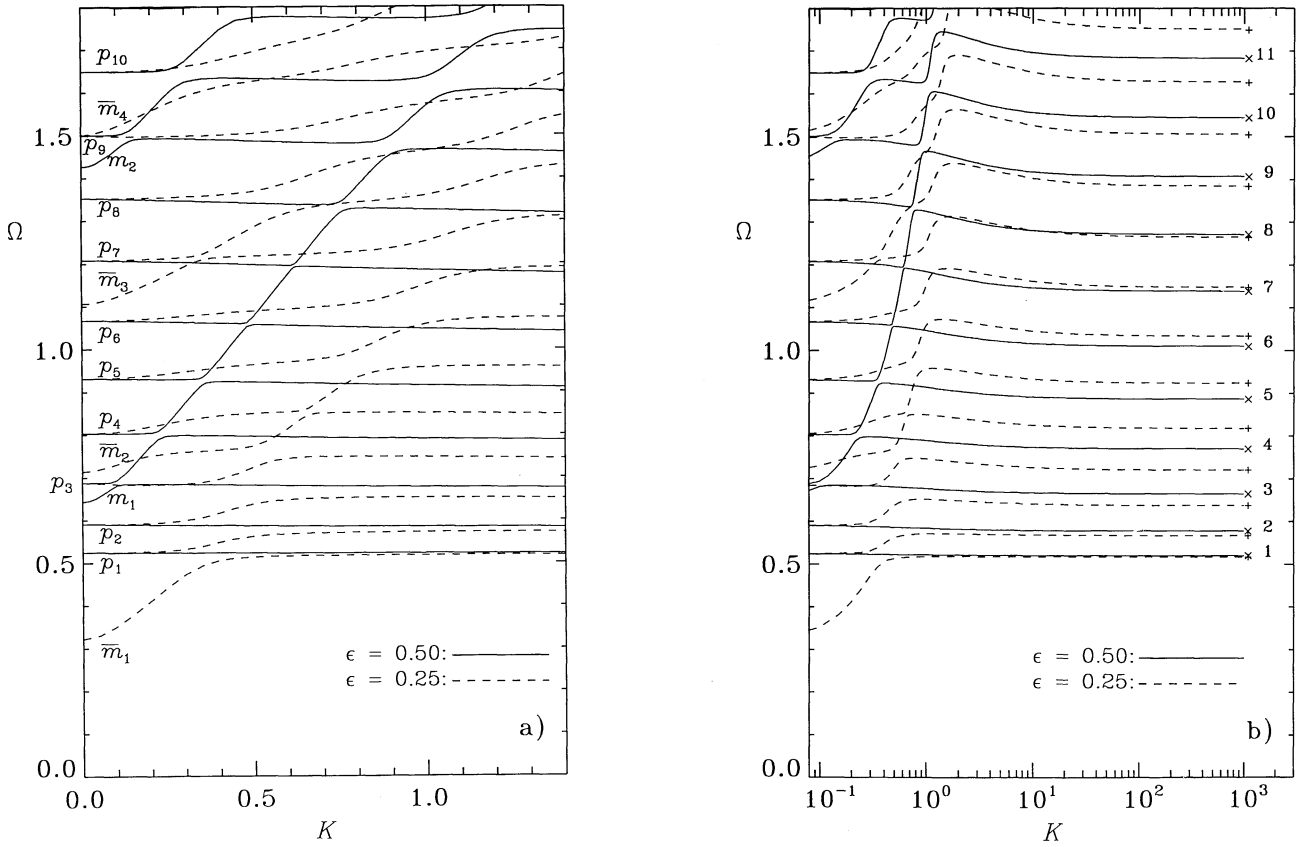

FIG. 10.—Variation of Ω with K in an isothermal atmosphere of extent $D = 20$, for $\epsilon = 0.5$ (*solid lines*) and $\epsilon = 0.25$ (*dashed lines*). In panel (*a*) the classification of the modes into m- and p-types refers to the solutions of eqs. (7) and (8), respectively, for $K = 0$. Note the avoided crossings between the p-like and magnetic modes. Panel (*b*) illustrates the behavior at moderate and large K. Here the frequencies resulting from solving eq. (9), valid in the limit $K \to \infty$, are marked with a cross (×) (for $\epsilon = 0.5$) and a plus (+) (for $\epsilon = 0.25$); the crosses have been labeled with the order of the corresponding modes.

strong-field case, the frequencies of the m-modes are given approximately by (Scheuer & Thomas 1981)

$$\Omega_{m,l} = \sqrt{\frac{\epsilon^2}{4} j_{2K,l}^2 + K^2}\,, \tag{53}$$

where $j_{2K,l}$ denotes the lth zero of J_{2K}. Hence, unlike the weak-field case, the m-mode frequencies increase roughly parabolically with K. On the other hand, the p-mode frequencies are essentially independent of K for small K. This is because, for these modes, $\xi_z \gg \xi_x$ (near $K \simeq 0$), so that ξ_z can be determined from equation (A32), with the right-hand side neglected. This solution is the same as equation (8) with eigenfrequencies given by equation (52), which are, of course, independent of K. For larger K, the frequencies decrease slightly with K. This behavior was also found by Abdelatif (1990) and is related to the fact that as K increases, the mode takes on the character of a slow magneto-acoustic wave. The latter mode has a small negative slope in the diagnostic diagram. This behavior leads to avoided crossings, which occur when the frequencies of the two sets of modes become close. Considering, for example, the m_1 mode. It undergoes an avoided crossing with the p_3 mode. As K increases further, a mode conversion occurs with a transformation of the p_3 mode into the m_1 mode and vice versa. The "new" m_1 mode undergoes avoided crossings with higher order p-modes, as can be seen quite clearly in both panels of Figure 10.

The effect of varying the magnetic field can be seen from the solutions with $\epsilon = 0.25$, also shown in Figures 10*a*–10*b*. It is evident that at $K = 0$, where the acoustic and magnetic modes are decoupled, the p-mode frequencies are the same as before; however, there are roughly twice as many magnetic modes as for $\epsilon = 0.5$. Otherwise the behavior is quite similar in the two cases, although the avoided crossings tend to be less sharply defined for $\epsilon = 0.25$ than for $\epsilon = 0.5$. It should also be noted that at $K = 0$, the frequencies of the m-modes are not limited to lie above the acoustic cutoff frequency, unlike those of the fast or p-like modes.

Finally, let us consider the nature of the solutions in the limit of large K, depicted in Figure 10*b*. As mentioned earlier, when $K \to \infty$, the frequency of the fast mode tends to infinity, so that the low-order modes in this limit are basically of the slow type, which travel roughly at the acoustic speed for $v_A/c_S \gg 1$. The latter condition is satisfied over most of the vertical extent, apart from the lower layers. When K is large, the two sets of curves practically coincide for low orders. These solutions can therefore be approximately regarded as slow modes. However, when n increases, the curves corresponding to $\epsilon = 0.25$ fall below those corresponding to $\epsilon = 0.5$, with the change in frequency increasing with n. This is because for large n the solutions are also influenced by physical conditions in the lower part of the atmosphere, where $v_A/c_S \sim 1$. Frequencies in this limit, obtained from numerical solution of equation (9), are indicated in Figure 10*b* by crosses labeled with the mode order for $\epsilon = 0.5$, and by pluses for $\epsilon = 0.25$. There is evidently excellent agreement between the solutions to the full fourth-order system of equations and those found from the limiting second-order system.

8. DISCUSSION

On the basis of quantitative calculations, the present analysis has brought out many interesting features of waves in stratified media. Inclusion of the variable structure of the atmosphere in the vertical direction is the key factor responsible for mode conversion, mode reflection as well as the presence of cutoff frequencies. In order to highlight the properties of the modes, it was found instructive to consider the solutions in the weak- and strong-field limits. The former condition is likely to be satisfied for instance in the deep subphotospheric layers of the Sun where $c_S \gg v_A$. Thus, waves propagating in the deeper layers can be studied in the weak-field approximation. An upward propagating wave, excited from below, becomes increasingly dominated by magnetic effects, as a result of the sharp increase of v_A with z. In regions where $v_A/c_S \ll 1$, the character of the wave can be analyzed in terms of elementary modes. For $K \sim 0$, the solutions consist of essentially accoustic and magnetic waves. At larger values of K, magnetically modified Lamb- and gravity-wave–like solutions are also possible. As the modes travel upward, into layers of the atmosphere where $v_A \sim c_S$, the situation becomes very complicated (Zhugzhda 1984). Wave solutions in the strong-field limit (corresponding to $v_A \gg c_S$) describe the modes in the higher layers, where only those waves with frequencies greater than the acoustic cutoff value can propagate. Therefore, an upward propagating wave, with $\Omega < \Omega_a$, will be reflected before it reaches the upper layers of the atmosphere. Thus, such layers act as a filter, allowing only those modes with frequencies greater than the acoustic cutoff to pass through.

The main emphasis of our work has been on the weak-field case, where $v_A \ll c_S$ throughout the layer. An important feature of our analysis is that it provides a fairly simple way to obtain the normal modes of an isothermal atmosphere with a vertical magnetic field. The general solutions involving Meijer functions are complicated and provide few clues about the physical nature of the waves. We have derived a dispersion relation which enables the normal modes of a system to be aproximately determined, as long as $\theta > 1$. A characteristic feature is the presence of a spectrum of predominantly magnetic modes, which becomes increasingly dense with decreasing field strength. In particular, there is the possibility of propagating waves and normal modes at frequencies intermediate between the acoustic cutoff frequency Ω_a and the buoyancy frequency Ω_{BV}. The frequency of the m_1 mode provides a lower limit on the possible frequencies of oscillation of the system. Thus the lowest-frequency g-modes are eliminated by the additional stiffness provided by the magnetic field.

Our analysis reveals the existence of a magnetic Lamb mode. In the absence of a magnetic field, it is straightforward to show from the linearized wave equations the existence of a solution for which $\Omega = K$, and with

$$\xi_x = Ce^{(1-1/\gamma)z/H}\,, \qquad \xi_z = 0\,,$$

where C is a constant. This solution, of course, does not satisfy our boundary conditions; but in the magnetic case the boundary conditions can be satisfied through the introduction of a small admixture of a magnetic mode. An analytic expression for the magnetic Lamb-mode frequency, showing the correction due to interaction with other modes does not appear to have been obtained before. However, the presence of this mode has been noted earlier by Antia & Chitre (1979), Cattaneo (1984) and Lou

(1990, 1991). The Lamb mode is not present in the solutions for moderate or strong field shown in Figure 10, which shows no indication of avoided crossings in the vicinity of $\Omega = K$. We speculate that it disappears by merging into the slow mode spectrum for small K and into the fast mode spectrum for large K.

We should also like to comment briefly on the fact that our solutions do not exhibit accidental degeneracy when the frequencies of different modes approach each other. The origin of this phenomenon can be traced to the dispersion relation. At such frequencies, the lowest-order approximation breaks down and the higher order terms, which couple the modes, have to be considered. This coupling is responsible for avoided crossings. This type of behavior has been known in atomic physics for a long time (e.g., von Neuman & Wigner 1929), and more recently it has been encountered in the study of solar and stellar global oscillations (e.g., Osaki 1975; Aizenman, Smeyers, & Wergert 1977; Christensen-Dalsgaard 1980) as well as in terrestrial problems (e.g., Jones 1970; Francis 1973); however, the presence of avoided crossings in connection with MAG waves appears to have been noticed only fairly recently (Hasan & Abdelatif 1990; Abdelatif 1990; Hasan 1991).

This behavior is contained in the asymptotic dispersion relation, equation (15), derived in § 5, and must be taken into account when evaluating asymptotic corrections to the frequencies. In particular, the simple expressions derived in § 5.2, which neglected the presence of other modes, become singular in the vicinity of the avoided crossings. A more complete treatment was given in § 5.3. To illustrate this asymptotic behavior, Figure 11 shows numerically computed frequencies in a small region around the p_1-mode for the default parameters ($\epsilon = 0.01$, $D = 1$, $\gamma = 5/3$), together with the two types of asymptotic frequencies. The singularities in the simple asymptotic frequency corrections near the avoided crossings are evident, as is the fact that the behavior in these regions is reasonably well described by the extended asymptotic treatment accounting for the presence of other modes. On the other hand, the latter treatment is necessarily local in nature and hence does not capture the overall behavior of the frequencies. Therefore, to obtain the complete picture both types of asymptotic description must be taken into account.

The asymptotic analysis shows that the behavior of the frequencies near the avoided crossings, including the minimum separation between the two branches of frequencies, scales with the frequency separation η between adjacent magnetic modes; η, in turn, is proportional to the magnetic field B. It follows that as B tends to zero the number of avoided crossings between any p-mode and the magnetic modes tends to infinity, whereas the fraction of the frequency interval which is affected by the avoided crossings is approximately constant. Hence the field-free case is not recovered in the limit $B \to 0$, which is therefore a singular limit. An analogous situation is obtained for the Lamb mode: here again the total extent of the region affected by avoided crossings tends to a constant as B tends to zero; but in the field-free case there is no Lamb mode satisfying the boundary conditions. That a singular limit should arise in this problem is hardly surprising, given that for $B = 0$ the order of the relevant differential equations is reduced from four to two. However, it would still be of some interest to investigate this behavior in more detail.

In order to view the present work in perspective, let us compare our results with those of previous calculations on modes in an isothermal atmosphere with a vertical magnetic field. Although FP were the first to investigate this problem, their calculations did not include the determination of the normal mode frequencies. This was first carried out by Uchida & Sakurai (1975), under the "quasi-Alfvén" approximation and more rigorously by Scheuer & Thomas (1981). The latter authors were essentially attempting to use a simplified isothermal model to determine approximate mode frequencies in the umbra of a sunspot. They concentrated on the m-modes which behave like fast modes in the layers where $v_A \gg c_S$; these modes are localized mainly to the photosphere, because they suffer sharp downward reflection due to the increase of the Alfvén speed with height. Since the m-modes are mainly transverse, the sequence of mode numbers used by Scheuer & Thomas was with respect to the number of nodes in the horizontal displacement. They did not give the full frequency spectrum; in particular, they omitted the p-mode like solutions, since they considered them irrelevant to the subject of their paper (J. H. Thomas, private communication). Wood (1990) tabulated complete sets of frequencies, but only corresponding to very few values of K ($K = 0.068$, 0.124, and 0.273). Extensive sets of modes for an isothermal atmosphere for the moderate- to strong-field case were obtained by Hasan & Abdelatif (1990) and Abdelatif (1990). Our $K - \Omega$ diagrams for the

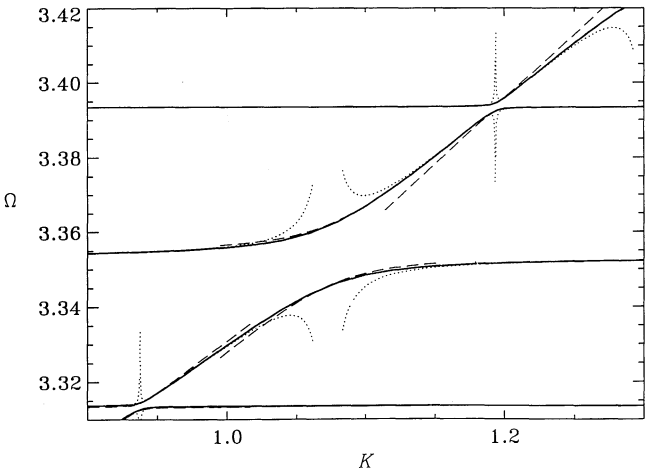

FIG. 11.—Details of avoided crossings in the diagnostic diagram between the p_1 mode and the magnetic modes, in an atmosphere with $\epsilon = 0.01$, $D = 1$, and $\gamma = 5/3$. The heavy continuous curves show the numerical solutions; the result of using the simple frequency corrections in eqs. (23) and (27) are shown as dotted curves, whereas asymptotic values based on taking the avoided crossings into account, as in eq. (38), are shown by dashed curves.

strong-field case (corresponding to $\epsilon = 0.5$) are similar to those given by Hasan & Abdelatif (1990) and Abdelatif (1990); they were shown basically to focus on mode classification and on the variation of the frequency in the limit of small and large horizontal wave number. Our aim was not to apply the results of an isothermal calculation to umbral oscillations, but rather to concentrate on the physical nature of waves in medium with a vertical magnetic field. Nevertheless, we should point out that avoided crossings in an isothermal atmosphere with a strong field were also examined by Abdelatif (1990) in terms of coupling between fast and slow modes. However, the weak-field limit was not considered in the latter paper.

An important aspect in the study of normal modes is the assumption about the boundary conditions. To illustrate the properties of the spectrum of oscillations in a mathematically well-defined case, we have chosen to enforce vanishing horizontal and vertical displacements at the top and bottom boundaries. In a realistic description of a stellar atmosphere more complex conditions would be involved. For instance, consider a vertical layer, which is forced at the top boundary. The downward propagating waves (for a weak field) can be analyzed in terms of a fast or p-like wave and a slow or m-like wave. If the temperature increases with depth, the former will be reflected, but the latter suffers only partial reflection, due to the decrease in Alfvén speed with depth. Consequently, the resulting cavity is imperfect, with degraded quality due to the loss of slow-mode energy at the bottom boundary. The nature of the $K - \Omega$ diagram also depends on the type of boundary conditions chosen. For the strong-field case, this was demonstrated explicitly by Abdelatif (1990), who found that the avoided crossings have a different form when gradients of displacements are set to zero at the boundaries, instead of the displacements themselves. In forthcoming papers, we expect to explore the nature of the solutions for different types of boundary conditions.

Last, we consider the question of wave classification. Our analysis has shown that in certain limits, it is possible to classify the wave solutions in terms of elementary modes of a stratified non-magnetic atmosphere or an unstratified atmosphere with a magnetic field. The limits corresponding to $K = 0$ and $K \to \infty$ provide a useful way to classify the modes. Our m-modes are simply the well-known slow modes in a weak field. For the most general case, the problem of mode classification is extremely difficult, especially when v_A/c_S changes by several orders of magnitudes over the vertical extent of the atmosphere. The stratification causes variation in the structure, which leads to mode conversion; hence, when analyzing MAG waves in terms of elementary modes, one should bear in mind that their behavior described in this way may be a local property. An alternative way of classifying modes, based on a Helmholtz decomposition of the displacements, was suggested by Hasan & Sobouti (1987) (see also Hasan & Abdelatif 1990 and Hasan 1991).

9. SUMMARY AND CONCLUSIONS

The main purpose of the present investigation was to extend the theory of MAG waves, by focusing on the effect of a vertical magnetic field on oscillations in a stratified atmosphere. Since the analysis of the general problem is rather complicated, it was found convenient, as a first step, to assume that the atmosphere is isothermal and that the magnetic field is uniform and of infinite horizontal extent. Although these assumptions are not generally valid, they nevertheless provide a starting point for a quantitative examination of MAG waves in stratified magnetized atmospheres. In order to obtain physical insight into the character of the solutions in regions where the Alfvén speed is much less than the sound speed, a weak-field approximation was used. The boundary conditions, although somewhat idealized, where made to simplify the mathematical analysis and to bring out the salient features associated with the effects of the magnetic field on the modal structure of the oscillations.

Several interesting features emerge from the calculations. The nature of the wave solutions depends upon the ratio of the Alfvén to sound speed in the atmosphere. It was found that in the weak-field limit, the oscillation spectrum could be analyzed in terms of the modes of a nonmagnetic stratified atmosphere and a magnetic mode (the slow MHD mode). For $K \sim 0$, only gravity-modified magnetic modes and p-modes are permitted. At moderate to large K, Lamb- and g-mode–like solutions are also possible. By using a perturbation expansion, we obtained the frequency corrections to the various modes due to mutual coupling with other modes. These corrections are valid as long as the frequencies of the individual modes are well separated. However, when the frequencies of two of the modes become close, there is strong mode coupling and *avoided crossings* occur. We examined the behavior of the solutions in the vicinity of these crossings and obtained expressions for the frequency separation of the modes. Detailed calculations in the form of diagnostic diagrams were presented. The effect of changing the field strength on the oscillation spectrum was also demonstrated.

We are grateful to H. A. B. Antia, B. L. Christensen-Dalsgaard, W. Kalkofen, K. Taulbjerg, and an anonymous referee for helpful comments and to D. O. Gough for providing us with a subroutine package for solving eigenvalue problems. This work was begun when one of us (J. C.-D.) visited the Tata Institute of Fundamental Research, Bombay in 1989 December. He wishes to express his gratitude to the Cambridge Society of Bombay for travel support. The computations reported here were supported in part by the Danish Natural Science Research Council. The work of S. S. H. was supported by grants from the Smithsonian Astrophysical Observatory and NASA through grant NAGW-1568. He is thankful to W. Kalkofen for his kind hospitality in Cambridge.

APPENDIX A

SOLUTION OF EQUATION (6)

1. GENERAL SOLUTION

Here we present the asymptotic properties of the solution of the wave equations in a uniform vertical magnetic field. It was shown by Zhugzhda & Dzhalilov (1982; ZD) that the general solution to equation (6) can be expressed in terms of Meijer functions as follows

$$\xi_x^{(h)} = G_{2,4}^{12}\left(\mu_h, \begin{matrix} a_1 & , & a_2 \\ \mu_1, \ \ldots, & \mu_i, \ldots, & \mu_4 \end{matrix} \middle| \theta^2\right) \qquad (i, h = 1, \ldots, 4;\ i \neq h)\,, \tag{A1}$$

where

$$\mu_{1,2} = \frac{(1 \pm i\alpha)}{2}, \qquad \mu_{3,4} = \pm K, \tag{A2}$$

$$a_{1,2} = \frac{(1 \pm \phi)}{2}, \tag{A3}$$

$$\alpha = \sqrt{4\Omega^2 - 1}, \tag{A4}$$

$$\phi = \sqrt{-\alpha^2 + 4K^2(1 - \Omega_{\rm BV}^2/\Omega^2)}, \tag{A5}$$

and $\Omega_{\rm BV}^2 = (\gamma - 1)/\gamma^2$ is the Brunt-Väisälä frequency (in dimensionless units).

Once $\xi_x^{(h)}$ is known, it is fairly straightforward to determine the corresponding solutions $\xi_z^{(h)}$ from either of equations (1) or (2). The complete solutions satisfying the required boundary conditions can be built up as linear combinations of $\xi_x^{(h)}$ and $\xi_z^{(h)}$.

2. STRONG FIELD SOLUTIONS

In the limit of a strong field, for which $c_S/v_A \ll 1$ and $\theta \ll 1$, the solutions are to lowest order in θ

$$\xi_x^{(h)} = R_h \theta^{2\mu_h} \qquad (h = 1, \ldots, 4), \tag{A6}$$

$$\xi_z^{(h)} = \begin{cases} R_h \dfrac{4i\Omega^2(\mu_h^2 - K^2)}{K(1/\gamma + \mu_h - 1)} \dfrac{\theta^{2\mu_h}}{4\theta^2} & (h = 1, 2), \\ -R_h \dfrac{iK[(\gamma - 1)/\gamma + \mu_h]}{(\mu_h^2 + \mu_h + \Omega^2)} \theta^{2\mu_h} & (h = 3, 4), \end{cases} \tag{A7}$$

where

$$R_h = \frac{\prod_{j=1}^{2} \Gamma(1 + \mu_h - a_j)}{\prod_{j=1, j\neq h}^{4} \Gamma(1 + \mu_h - \mu_j)}. \tag{A8}$$

When $\alpha^2 < 0$ ($\Omega^2 < \frac{1}{4}$), the amplitudes given by equations (A6)–(A7) either fall off or increase exponentially with height. Purely growing solutions are unphysical and can be discarded. The only permitted solutions correspond to evanescent waves. Hence, the atmosphere has a cutoff frequency, which is the same as the usual acoustic cutoff frequency ($\Omega_a = \frac{1}{2}$) in an unmagnetized atmosphere. On the other hand, for $\Omega > \Omega_a$, the solutions represent propagating waves.

3. WEAK FIELD SOLUTIONS

We now focus our attention on the opposite limit of a weak field, for which $c_S/v_A \gg 1$ and $\theta \gg 1$. This corresponds to the limit of small ϵ, with

$$\epsilon \equiv \frac{v_{A,0}}{c_S}. \tag{A9}$$

However, in addition we must require that the vertical extension d of the layer is not too large (see eq. [5c]) (for $d > 0$). Since the density increases for negative z, the above restriction, of course, does not apply if d lies below the plane $z = 0$.

When $\theta \gg 1$, the Meijer function in equation (A1) has the following asymptotic expansion (ZD):

$$G_{2,4}^{1,2}(\mu_h | \theta^2) = \frac{1}{2\sqrt{\pi\theta}} \left[e^{i(2\theta - \delta_h)} \left(1 + i\frac{M}{\theta} - \frac{M_1}{\theta^2}\right) + e^{-i(2\theta/\delta_h)} \left(1 - i\frac{M}{\theta} - \frac{M_1}{\theta^2}\right) \right] + \frac{1}{\theta} \left[S_h \left(1 + \frac{L_1^+}{\theta^2}\right) \theta^{2iK_z} + T_h \left(1 + \frac{L_1^-}{\theta^2}\right) \theta^{-2iK_z} \right] + O\left(\frac{1}{\theta^3}\right), \tag{A10}$$

where

$$K_z^2 = \Omega^2 - K^2 \left(1 - \frac{\Omega_{\rm BV}^2}{\Omega^2}\right) - \frac{1}{4} = \frac{\phi}{2i}, \tag{A11}$$

$$\delta_h = \pi(\tfrac{1}{4} + \mu_h), \tag{A12}$$

$$M = K^2 \frac{\Omega_{\rm BV}^2}{\Omega^2} - \frac{1}{16}, \tag{A13}$$

$$M_1 = \frac{K^2}{2} - \frac{1}{32} + \frac{M}{4}(2M - 3), \tag{A14}$$

$$L_1^{\pm} = -\frac{[w_\pm(w_\pm + 1) + \Omega^2](w_\pm^2 - K^2)}{2w_\pm}, \tag{A15}$$

$$w_{\pm} = \tfrac{1}{2} \mp iK_z = a_{2,1}\,, \tag{A16}$$

$$S_h = \frac{\Gamma(\phi)\Gamma(1+\mu_h-a_1)}{\prod_{j=1,j\neq h}^{4}\Gamma(a_1-\mu_j)}\,, \tag{A17}$$

$$T_h = \frac{\Gamma(-\phi)\Gamma(1+\mu_h-a_2)}{\prod_{j=1,j\neq h}^{4}\Gamma(a_2-\mu_j)}\,. \tag{A18}$$

It should be borne in mind that the expansion for the Meijer function given by equation (A10) is valid as long as $M/\theta \ll 1$, which restricts K to values such that $K^2 \ll \Omega^3\, v_A/c_s$. Thus, for $K \sim 1$, we have the condition $v_A/c_s \ll \Omega^3$, which places a more severe restriction on the permitted field strengths than the condition $\theta \gg 1$.

Using the expansion given by equation (A10), we find that $\xi_x^{(h)}$ can be expressed in a compact form as follows

$$\xi_x^{(h)} = \frac{1}{\theta}\sum_{j=1}^{2} C_j^{(h)} f_j(\theta) + \frac{1}{\sqrt{\theta}}\sum_{j=3}^{4} C_j^{(h)} f_j(\theta)\,, \tag{A19}$$

where

$$C_1^{(h)} = T_h + S_h\,, \qquad C_2^{(h)} = T_h - iS_h\,, \tag{A20}$$

$$C_3^{(h)} = \frac{1}{\sqrt{\pi}}\sin\delta_h\,, \qquad C_4^{(h)} = \frac{1}{\sqrt{\pi}}\cos\delta_h\,. \tag{A21}$$

The functions f_j are

$$f_1 = \left(q_1 + \frac{q_1'}{\theta^2}\right)\cos K_z Z - \left(q_2 + \frac{q_2'}{\theta^2}\right)\sin K_z Z + O\left(\frac{1}{\theta^3}\right), \tag{A22}$$

$$f_2 = \left(q_1 + \frac{q_1'}{\theta^2}\right)\sin K_z Z + \left(q_2 + \frac{q_2'}{\theta^2}\right)\cos K_z Z + O\left(\frac{1}{\theta^3}\right), \tag{A23}$$

$$f_3 = \left(1 - \frac{M_1}{\theta^2}\right)\cos 2\theta - \frac{M}{\theta}\sin 2\theta + O\left(\frac{1}{\theta^3}\right), \tag{A24}$$

$$f_4 = \left(1 - \frac{M_1}{\theta^2}\right)\sin 2\theta + \frac{M}{\theta}\cos 2\theta + O\left(\frac{1}{\theta^3}\right), \tag{A25}$$

where $Z = z/H$ and

$$q_1 = \frac{1}{2}\left[\left(\frac{\Omega}{\epsilon}\right)^{-2iK_z} + \left(\frac{\Omega}{\epsilon}\right)^{2iK_z}\right], \tag{A26}$$

$$q_2 = \frac{1}{2i}\left[\left(\frac{\Omega}{\epsilon}\right)^{-2iK_z} - \left(\frac{\Omega}{\epsilon}\right)^{2iK_z}\right], \tag{A27}$$

$$q_1' = \frac{1}{2}\left[L_1^{-}\left(\frac{\Omega}{\epsilon}\right)^{-2iK_z} + L_1^{+}\left(\frac{\Omega}{\epsilon}\right)^{2iK_z}\right], \tag{A28}$$

$$q_2' = \frac{1}{2i}\left[L_1^{-}\left(\frac{\Omega}{\epsilon}\right)^{-2iK_z} - L_1^{+}\left(\frac{\Omega}{\epsilon}\right)^{2iK_z}\right]. \tag{A29}$$

It follows that to this asymptotic order the general solution ξ_x, which is a linear combination of the $\xi_x^{(h)}$, may equally well be expressed as a linear combination of the functions f_j ($j = 1, \ldots, 4$). Physically, $f_{1,2}$ and $f_{3,4}$ correspond to the nonmagnetic and magnetic contributions to the solution, respectively. In order to calculate $\xi_z^{(h)}$, we assume a series expansion in ascending powers of $1/\theta$, similar to $\xi_x^{(h)}$ but with different coefficients. It turns out that $\xi_z^{(h)}$ can be expressed as

$$i\xi_z^{(h)} = \frac{1}{\theta}\sum_{j=1}^{2} C_j^{(h)} g_j(\theta) + \frac{1}{\theta^{3/2}}\sum_{j=3}^{4} C_j^{(h)} g_j(\theta)\,. \tag{A30}$$

The coefficients $g_{3,4}$ and $g_{1,2}$ in equation (A30) are the corresponding magnetic and nonmagnetic contributions to ξ_z respectively. These can be determined from equations (1) and (2), respectively, rewritten as

$$\left[4(\Omega^2 - K^2)\theta^2 - 4\Omega^2K^2 + \Omega^2\theta\frac{d}{d\theta} + \Omega^2\theta^2\frac{d^2}{d\theta^2}\right]\xi_x = -4iK\theta^2\left(\frac{1}{\gamma} + \frac{\theta}{2}\frac{d}{d\theta}\right)\xi_z\,, \tag{A31}$$

$$\left[\Omega^2 + \frac{3}{4}\theta\frac{d}{d\theta} + \frac{\theta^2}{4}\frac{d^2}{d\theta^2}\right]\xi_z = -iK\left(\frac{\gamma-1}{\gamma} + \frac{\theta}{2}\frac{d}{d\theta}\right)\xi_x\,. \tag{A32}$$

The functions g_j, ($g_j = 1, \ldots, 4$) are

$$g_1 = \left(p_1 + \frac{p_1'}{\theta^2}\right) \cos K_z Z - \left(p_2 + \frac{p_2'}{\theta^2}\right) \sin K_z Z + O\left(\frac{1}{\theta^3}\right), \tag{A33}$$

$$g_2 = \left(p_1 + \frac{p_1'}{\theta^2}\right) \sin K_z Z + \left(p_2 + \frac{p_2'}{\theta^2}\right) \cos K_z Z + O\left(\frac{1}{\theta^3}\right), \tag{A34}$$

$$g_3 = K\left(\sin 2\theta + \frac{N}{\theta} \cos 2\theta\right) + O\left(\frac{1}{\theta^2}\right), \tag{A35}$$

$$g_4 = K\left(-\cos 2\theta + \frac{N}{\theta} \cos 2\theta\right) + O\left(\frac{1}{\theta^2}\right). \tag{A36}$$

Here

$$p_1 = \frac{K}{2}\left[Q_0^-\left(\frac{\Omega}{\epsilon}\right)^{-2iK_z} + Q_0^+\left(\frac{\Omega}{\epsilon}\right)^{2iK_z}\right], \tag{A37}$$

$$p_2 = \frac{K}{2i}\left[Q_0^-\left(\frac{\Omega}{\epsilon}\right)^{-2iK_z} - Q_0^+\left(\frac{\Omega}{\epsilon}\right)^{2iK_z}\right], \tag{A38}$$

$$p_1' = \frac{K}{2}\left[Q_1^-\left(\frac{\Omega}{\epsilon}\right)^{-2iK_z} + Q_1^+\left(\frac{\Omega}{\epsilon}\right)^{2iK_z}\right], \tag{A39}$$

$$p_2' = \frac{K}{2i}\left[Q_1^+\left(\frac{\Omega}{\epsilon}\right)^{-2iK_z} - Q_1^-\left(\frac{\Omega}{\epsilon}\right)^{2iK_z}\right], \tag{A40}$$

where

$$N = M + \frac{1}{\gamma} + \frac{1}{4} - \frac{\Omega^2}{K^2}, \tag{A41}$$

$$Q_0^{\pm} = -\frac{i}{r} t_{\pm}, \tag{A42}$$

$$t_{\pm} = \pm K_z + i\left(\frac{1}{\gamma} - \frac{1}{2}\right), \tag{A43}$$

$$Q_1^{\pm} = \frac{(w_{\pm} + 1/\gamma)(w_{\pm}^2 - K^2)}{2w_{\pm}}, \tag{A44}$$

$$r = K^2\left(1 - \frac{\Omega_{BV}^2}{\Omega^2}\right). \tag{A45}$$

APPENDIX B

DERIVATION OF THE DISPERSION RELATION (15)

Applying the boundary conditions given by equation (14) to equations (A19) and (A30) yields a set of four equations which can be written as

$$AX = 0, \tag{B1}$$

where

$$X^T = (C_1 \quad C_2 \quad C_3 \quad C_4),$$

$$A = \begin{pmatrix} \frac{f_1(0)}{\theta_0} & \frac{f_2(0)}{\theta_0} & \frac{f_3(0)}{\sqrt{\theta_0}} & \frac{f_4(0)}{\sqrt{\theta_0}} \\ \frac{f_1(D)}{\theta_D} & \frac{f_2(D)}{\theta_D} & \frac{f_3(D)}{\sqrt{\theta_D}} & \frac{f_4(D)}{\sqrt{\theta_D}} \\ \frac{g_1(0)}{\theta_0} & \frac{g_2(0)}{\theta_0} & \frac{g_3(0)}{\theta_0^{3/2}} & \frac{g_4(0)}{\theta_0^{3/2}} \\ \frac{g_1(D)}{\theta_D} & \frac{g_2(D)}{\theta_D} & \frac{g_3(D)}{\theta_D^{3/2}} & \frac{g_4(D)}{\theta_D^{3/2}} \end{pmatrix}. \tag{B2}$$

Here $\theta_0 = \theta(0)$ and $\theta_D = \theta(D)$. The condition for equation (B1) to have a nontrivial solution is

$$\det [A] = 0 . \tag{B3}$$

Expanding equation (B3), we have

$$\frac{(f_{30} f_{4D} - f_{3D} f_{40})}{\sqrt{\theta_0 \theta_D}} \frac{(g_{10} g_{2D} - g_{1D} g_{20})}{\theta_0 \theta_D} + \frac{(f_{3D} g_{4D} - g_{3D} f_{4D})}{\theta_D^2} \frac{(g_{10} f_{20} - g_{10} f_{20})}{\theta_0^2}$$
$$+ \frac{(f_{3D} g_{40} - g_{30} f_{4D})}{\theta_0^{3/2} \theta_D^{1/2}} \frac{(f_{10} g_{2D} - g_{1D} f_{20})}{\theta_0 \theta_D} + \frac{(f_{30} g_{40} - g_{30} f_{40})}{\theta_0^2} \frac{(g_{1D} f_{2D} - f_{1D} g_{2D})}{\theta_D^2}$$
$$+ \frac{(f_{30} g_{4D} - g_{3D} f_{40})}{\theta_0^{1/2} \theta_D^{3/2}} \frac{(f_{1D} g_{20} - g_{10} f_{2D})}{\theta_0 \theta_D} + \frac{(g_{30} g_{4D} - g_{3D} g_{40})}{\theta_0^{3/2} \theta_D^{3/2}} \frac{(f_{10} f_{2D} + f_{1D} f_{20})}{\theta_0 \theta_D} = 0 , \tag{B4}$$

where $f_{10} \equiv f_1(0)$ and so on. Substituting for f_j and g_j ($j = 1, \ldots, 4$) from equations (A22)–(A25) and (A33)–(A36), respectively, we have

$$f_{30} f_{4D} - f_{3D} f_{40} = -\sin \tilde{\theta} + \left(\frac{1}{\theta_D} - \frac{1}{\theta_0}\right) M \cos \tilde{\theta} - \frac{1}{\theta_0 \theta_D} M^2 \sin \tilde{\theta} + \left(\frac{1}{\theta_D^2} + \frac{1}{\theta_0^2}\right) M_1 \sin \tilde{\theta} + O\left(\frac{1}{\theta^3}\right), \tag{B5}$$

$$f_{3D} g_{4D} - g_{3D} f_{4D} = -K + O\left(\frac{1}{\theta^2}\right), \tag{B6}$$

$$f_{30} g_{40} - g_{30} f_{40} = -K + O\left(\frac{1}{\theta^2}\right), \tag{B7}$$

$$f_{3D} g_{40} - g_{30} f_{4D} = -K\left[\cos \tilde{\theta} + \left(\frac{M}{\theta_D} - \frac{N}{\theta_0}\right) \sin \tilde{\theta}\right] + O\left(\frac{1}{\theta^2}\right), \tag{B8}$$

$$f_{30} g_{4D} - g_{3D} f_{40} = -K\left[\cos \tilde{\theta} - \left(\frac{M}{\theta_0} - \frac{N}{\theta_D}\right) \sin \tilde{\theta}\right] + O\left(\frac{1}{\theta^2}\right), \tag{B9}$$

$$g_{30} g_{4D} - g_{3D} g_{40} = -K^2 \sin \tilde{\theta} + O\left(\frac{1}{\theta}\right), \tag{B10}$$

$$g_{10} g_{2D} - g_{1D} g_{20} = U \sin K_z D + \left(\frac{1}{\theta_D^2} + \frac{1}{\theta_0^2}\right) V_1 \sin K_z D + \left(\frac{1}{\theta_D^2} - \frac{1}{\theta_0^2}\right) W_1 \cos K_z D + O\left(\frac{1}{\theta^4}\right), \tag{B11}$$

$$g_{10} f_{20} - f_{10} g_{20} = W + O\left(\frac{1}{\theta^2}\right), \tag{B12}$$

$$f_{10} g_{2D} - g_{1D} f_{20} = -W \cos K_z D + V \sin K_z D + O\left(\frac{1}{\theta^2}\right), \tag{B13}$$

$$g_{1D} f_{2D} - f_{1D} g_{2D} = W + O\left(\frac{1}{\theta^2}\right), \tag{B14}$$

$$f_{1D} g_{20} - g_{10} f_{2D} = -W \cos K_z D - V \sin K_z D + O\left(\frac{1}{\theta^2}\right), \tag{B15}$$

$$f_{10} f_{2D} - f_{1D} f_{20} = \sin K_z D + O\left(\frac{1}{\theta^2}\right). \tag{B16}$$

Here $\tilde{\theta} = \theta_D - \theta_0$, and M, M_1, and N are defined in equations (A13), (A14), and (A41), respectively; also

$$U = p_1^2 + p_2^2 = \frac{(\Omega^2 - K^2)}{r}, \tag{B17}$$

$$W = p_1 q_2 - p_2 q_1 = \frac{K K_z}{r}, \tag{B18}$$

$$V = p_1 q_1 + p_2 q_2 = \frac{K}{r}\left(\frac{1}{2} - \frac{1}{\gamma}\right), \tag{B19}$$

$$W_1 = p_1 p_2' - p_2 p_1' = -\frac{K^2}{r} u_- , \tag{B20}$$

$$V_1 = p_1 p_2' - p_2 p_1' = -\frac{K^2}{ir}\, u_+ , \tag{B21}$$

$$u_\pm = \tfrac{1}{2}(t_- Q_1^+ \pm t_+ Q_1^-) . \tag{B22}$$

Substituting equations (B5)–(B16) into equation (B4) yields

$$\begin{aligned}
&-U \sin\tilde{\theta} \sin K_z D + \left(\frac{1}{\theta_D} - \frac{1}{\theta_0}\right) MU \sin K_z D \cos\tilde{\theta} - \frac{1}{\theta_0\theta_D} M^2 U \sin\tilde{\theta} \sin K_z D \\
&+ \left(\frac{1}{\theta_D^2} + \frac{1}{\theta_0^2}\right)(M_1 U - V_1) \sin\tilde{\theta} \sin K_z D - \left(\frac{1}{\theta_D^2} - \frac{1}{\theta_0^2}\right) W_1 \sin\tilde{\theta} \cos K_z D \\
&- \frac{2}{\sqrt{\theta_0\theta_D}} KW + \left(\frac{1}{\theta_D} + \frac{1}{\theta_0}\right) KW \cos K_z D \cos\tilde{\theta} + \left(\frac{1}{\theta_D} - \frac{1}{\theta_0}\right) KV \cos\tilde{\theta} \sin K_z D \\
&+ \left(\frac{1}{\theta_D^2} - \frac{1}{\theta_0^2}\right) KWN \sin\tilde{\theta} \cos K_z D - \frac{2}{\theta_0\theta_D} KVM \sin\tilde{\theta} \sin K_z D \\
&+ \left(\frac{1}{\theta_D^2} + \frac{1}{\theta_0^2}\right) KVN \sin\tilde{\theta} \sin K_z D - \frac{1}{\theta_0\theta_D} K^2 \sin\tilde{\theta} \sin K_z D + O\left(\frac{1}{\theta^3}\right) = 0 .
\end{aligned} \tag{B23}$$

Finally, by substituting equations (B17)–(B21) into equation (B23), we obtain

$$\begin{aligned}
(\Omega^2 - K^2) \sin\tilde{\theta} \sin (K_z D) = 2\,\frac{\epsilon}{\Omega}\, e^{D/4} \Bigg\{ & K_z K^2 \left[\cosh\left(\frac{D}{4}\right) \cos\tilde{\theta} \cos (K_z D) - 1 \right] \\
& + \sinh\left(\frac{D}{4}\right) \cos\tilde{\theta} \sin (K_z D) \left[M(\Omega^2 - K^2) - K^2 \left(\frac{1}{\gamma} - \frac{1}{2}\right) \right] \Bigg\} \\
& + \frac{\epsilon^2}{\Omega^2}\, e^{D/2} \sin\tilde{\theta} \Bigg\{ \left[M^2(K^2 - \Omega^2) + 2MK^2 \left(\frac{1}{\gamma} - \frac{1}{2}\right) - rK^2 \right] \sin (K_z D) \\
& + 2K^2 (u_- + NK_z) \sinh\left(\frac{D}{2}\right) \cos (K_z D) \\
& + 2[M_1(\Omega^2 - K^2) - iK^2 u_+] \cosh\left(\frac{D}{2}\right) \sin (K_z D) \Bigg\} + O\left(\frac{\epsilon^3}{\Omega^3}\right) ,
\end{aligned} \tag{B24}$$

which is the dispersion relation accurate to second order in ϵ.

REFERENCES

Abdelatif, T. E. 1990, Sol. Phys., 129, 201
Abdelatif, T. E., Lites, B. W., & Thomas, J. H. 1984, in Small-Scale Dynamical Processes in Solar and Stellar Atmospheres, ed. S. L. Keil (Sunspot: Sacramento Peak Obs.), 141
———. 1986, ApJ, 311, 1015
Aizenman, M. L., Smeyers, P., & Weigert, A. 1977, A&A, 58, 41
Antia, H., & Chitre, S. M. 1979, Sol. Phys., 63, 67
Balthasar, H., Küveler, G., & Wiehr, E. 1987, Sol. Phys., 112, 39
Beckers, J. M., & Schulz, R. B. 1972, Sol. Phys., 27, 61
Bel, N., & Mein, P. 1971, A&A, 11, 234
Bhatnagar, A., Livingston, W. C., & Harvey, J. W. 1972, Sol. Phys., 27, 80
Bironi, D., Goosens, M., Cousens, A., & Mestel, L. 1982, MNRAS, 201, 619
Bogdan, T. J., & Cattaneo, F. 1989, ApJ, 342, 545
Bogdan, T. J., & Zweibel, E. G. 1987, ApJ, 318, 888
Campbell, W. R., & Roberts, B. 1989, ApJ, 338, 538
Campos, L. M. B. C. 1985, Rev. Mod. Phys., 59, 363
Cash, J. R., & Moore, D. R. 1980, Bol. Inst. Tonantzintla, 20, 44
Cattaneo, F. 1984, Ph.D. thesis, Darwin College, Cambridge
Christensen-Dalsgaard, J. 1980, MNRAS, 190, 765
Dziembowski, W. A., & Goode, P. R. 1984, Mem. Soc. Astr. Ital., 55, 185
Ferraro, V. C., & Plumpton, C. 1958, ApJ, 129, 459 (FP)
Francis, S. H. 1973, J. Geophys. Res., 78, 2278
Friedrich, H., & Wintgen, D. 1989, Phys. Rep., 183, 37
Giovanelli, R. G. 1975, Sol. Phys., 44, 289
Giovanelli, R. G., Harvey, J. W., & Livingston, W. C. 1978, Sol. Phys., 59, 40
Goosens, M. 1972, Ap&SS, 16, 386
Goosens, M., Smeyers, P., & Denis, J. 1976, Ap&SS, 39, 257
Gough, D. O., & Taylor, P. P. 1984, Mem. Soc. Astr. Ital., 55, 215
Gough, D. O., & Thompson, M. J. 1988, in IAU Symp. 123, Advances in Helio- and Astroseismology, ed. J. Christensen-Dalsgaard & S. Frandsen (Dordrecht: Reidel), 155
———. 1990, MNRAS, 242, 25
Gurman, J. B. 1987, Sol. Phys., 108, 61
Hasan, S. S. 1991, ApJ, 366, 328
Hasan, S. S., & Abdelatif, T. 1990, in Physics of Magnetic Flux Ropes, ed. C. T. Russell, E. R. Priest, & L. C. Lee (Washington, DC: AGU Monograph), 93
Hasan, S. S., & Sobouti, Y. 1987, MNRAS, 228, 427
Hollweg, J. V. 1990, in Physics of Magnetic Flux Ropes, ed. C. T. Russell, E. R. Priest, & L. C. Lee (Washington, DC: AGU Monograph), 23
Jones, W. L. 1970, J. Atm. Terr. Phys. 32, 1555
Lamb, H., 1932, Hydrodynamics (6th ed.; Cambridge Univ. Press)
Ledoux, P., & Simon, R. 1957, A&A, 20, 185
Leibacher, J. W., & Stein, R. F. 1981, in The Sun as a Star, ed. S. Jordan (Washington, DC: NASA), 263
Leroy, B., & Schwartz, S. J. 1982, A&A, 112, 84
Lites, B. W. 1984, ApJ, 277, 874
Lites, B. W., & Thomas, J. H. 1985, ApJ, 294, 682
Lou, Y. L. 1990, ApJ, 361, 527
———. 1991, ApJ, 367, 367
McLellan, A., & Winterberg, F. 1968, Sol. Phys., 4, 401
Moore, R. L., & Rabin, D. 1985, ARA&A, 23, 239
Moreno-Insertis, F., & Spruit, H. C. 1989, ApJ, 342, 1158
Nagakawa, Y., Priest, E. R., & Wellck, R. E. 1973, ApJ, 184, 931
Osaki, Y. 1975, PASJ, 27, 237
Rice, J. B., & Gaizauskas, V. 1973, Sol. Phys., 32, 421
Roberts, B. 1985, in Solar System Magnetic Fields, ed. E. R. Priest (Dordrecht: Reidel), 37
Roberts, B. 1990, in Physics of Magnetic Flux Ropes, ed. C. T. Russell, E. R. Priest, & L. C. Lee (Washington, DC: AGU Monograph), 113
Roberts, B., & Campbell, W. R. 1986, Nature, 323, 603
Roberts, B., & Small, L. 1990, preprint
Roberts, P. H., & Soward, A. M. 1983, MNRAS, 205, 1171
Scheuer, M. A., & Thomas, J. H. 1981, Sol. Phys., 71, 21
Schröter, E. H., & Soltau, D. 1981, A&A, 49, 463

Spruit, H. C., & Bogdan, T. J. 1992, preprint
Thomas, J. H. 1982, ApJ, 262, 760
———. 1983, Ann. Rev. Fluid Mech., 15, 321
———. 1990, in Physics of Magnetic Flux Ropes, ed. C. T. Russell, E. R. Priest, & L. C. Lee (Washington, DC: AGU Monograph), 133
Uchida, Y., & Sakurai, T. 1975, PASJ, 27, 259
von Neuman, J., & Wigner, E., 1929, Phys. Z., 30, 465
von Uexküll, M., Kneer, F., & Matting, W. 1983, A&A, 123, 263
Vorontsov, S. V. 1988, in IAU Symp. 123, Advances in Helio- and Astroseismology, ed. J. Christensen-Dalsgaard & S. Frandsen (Dordrecht: Reidel), 151
Wood, W. P. 1990, Sol. Phys., 128, 353
Zhugzhda, Yu. D. 1979, Soviet Astron., 23, 42
———. 1984, MNRAS, 207, 731
Zhugzhda, Yu. D., & Dzhalilov, N. S. 1982, A&A, 112, 16
———. 1984a, A&A, 132, 45
Zhugzhda, Yu. D., & Dzhalilov, N. S. 1984b, A&A, 132, 52
Zweibel, E. G., & Bogdan, T. J. 1986, ApJ, 308, 401